Journal of Computational Physics 259 (2014), pp. 51–69.

Electron and Ion Transport Equations in Computational Weakly-Ionized Plasmadynamics

Bernard Parent[*], Sergey O. Macheret[†], and Mikhail N. Shneider[‡]

A new set of ion and electron transport equations is proposed to simulate steady or unsteady quasi-neutral or non-neutral multicomponent weakly-ionized plasmas through the drift-diffusion approximation. The proposed set of equations is advantaged over the conventional one by being considerably less stiff in quasi-neutral regions because it can be integrated in conjunction with a potential equation based on Ohm's law rather than Gauss's law. The present approach is advantaged over previous attempts at recasting the system by being applicable to plasmas with several types of positive ions and negative ions and by not requiring changes to the boundary conditions. Several test cases of plasmas enclosed by dielectrics and of glow discharges between electrodes show that the proposed equations yield the same solution as the standard equations but require 10 to 100 times fewer iterations to reach convergence whenever a quasi-neutral region forms. Further, several grid convergence studies indicate that the present approach exhibits a higher resolution (and hence requires fewer nodes to reach a given level of accuracy) when ambipolar diffusion is present. Because the proposed equations are not intrinsically linked to specific discretization or integration schemes and exhibit substantial advantages with no apparent disadvantage, they are generally recommended as a substitute to the fluid models in which the electric field is obtained from Gauss's law as long as the plasma remains weakly-ionized and unmagnetized.

1. Introduction

WEAKLY-IONIZED plasmas have recently been the focus of increased attention as a means to improve the capabilities of aircraft. Possible applications of weakly-ionized plasmas that are currently under investigation include (and are not limited to) boundary layer control on fixed and rotating wings using DBD plasma actuators, power generation on board high-speed airbreathing vehicles through MHD generators, or thrust production using MHD accelerators. Numerical simulations of weakly-ionized airflow for aerospace applications have so far been accomplished mostly using a fluid model (i.e. the drift-diffusion approximation) [1, 2, 3, 4] because more involved physical models based on kinetic theory require excessive computational resources at the relatively high densities encountered in plasma aerodynamics, although some progress is being made in this area [5].

When discretized using finite-difference stencils, the drift-diffusion model in which the potential equation is obtained from Gauss's law is well known to be particularly stiff. (A stiff system of equations here denotes a system for which the integration steplength is forced to be excessively small in relation to the smoothness of the exact solution.) The stiffness becomes particularly severe in the quasi-neutral regions where the positive charge density approaches closely the negative charge density. To relieve the stiffness of the system, a strategy was proposed recently in which the potential equation is obtained from Ohm's law rather than Gauss's law (see Ref. [6] and also Ref. [7]). To ensure that Gauss's law is satisfied in the non-neutral regions, some source terms are added to the ion conservation equation. In doing so, it was possible to specify a considerably larger integration steplength, and this lead to a hundredfold reduction in the number of iterations to reach convergence whenever the plasma had some regions that were quasi-neutral. Further, it was demonstrated that such a gain in convergence acceleration

[*]Faculty Member, Dept. of Aerospace Engineering, Pusan National University, Busan 609-735, Korea, http://www.bernardparent.com.

[†]Senior Research Scientist, Dept. of Mechanical and Aerospace Engineering, Princeton University, Princeton, NJ 08544-5263, USA. Current address: Lockheed Martin Aeronautics Company, 1011 Lockheed Way, Palmdale, California 93599-0160

[‡]Senior Research Scientist, Dept. of Mechanical and Aerospace Engineering, Princeton University, Princeton, NJ 08544-5263, USA.

could be obtained with no loss in accuracy: either on coarse or fine meshes, the solution obtained with a potential based on Ohm's law had a numerical error that was not greater than the one obtained with a potential based on Gauss's law.

Nonetheless, the recast set of equations presented in Ref. [6] does have one drawback over the conventional set when simulating weakly-ionized plasmas. Namely, the boundary condition at the anode needs to be redefined or Gauss's law would not be satisfied within the anode sheath close to the surface. This is problematic because the redefined boundary condition is approximate and it is uncertain whether it would remain valid in the general case. Further, the approach presented in Ref. [6] is limited to a three-component plasma (one type of positive ions, electrons, and neutrals) in one dimension, and it is not clear how it could be extended to multidimensional and multicomponent plasmas (plasmas with several types of positive ions and negative ions).

The goal of this paper is to build upon the ideas presented in Ref. [6] and to derive a new set of electron and ion transport equations that is more computationally efficient than the conventional set and that is generally applicable to multidimensional and multicomponent weakly-ionized plasma flows. In addition, in contrast to the approach shown in [6], we aim to find a formulation that can be used without modifying the boundary conditions at the electrodes.

This paper is divided as follows: first, we provide a description of the physical model suitable to multicomponent and multidimensional weakly-ionized plasmas; this is followed by the outline of the "conventional governing equations" (i.e., the set of equations that is normally used to simulate weakly-ionized plasmas using a fluid model), and then by the proposed recast of the electron and ion equations; a short summary is then given of the discretization and integration schemes used herein; finally, some test cases are presented typical of weakly-ionized plasmas encountered in plasma aerodynamics, and the performance of the proposed set of equations is assessed in terms of the number of iterations needed to reach convergence and of the resolution of the converged solution.

2. Physical Model

In this section, a short outline is given of the fluid model that is generally used to simulate weakly-ionized plasmas (i.e., plasmas with an ionization fraction less than 0.001 or so). Commonly referred to as the "drift-diffusion model" the physical model considered is widely used to simulate weakly-ionized plasmas not only for steady cases but also for unsteady cases in which the displacement current is not negligible (see for instance Refs. [8, 9, 10, 11, 12, 13, 14, 15]).

Conservation of mass entails the following transport equation for each charged species:

$$\frac{\partial N_k}{\partial t} + \sum_{i=1}^{3} \frac{\partial}{\partial x_i}(N_k \boldsymbol{V}_i^k) = W_k \tag{1}$$

with N_k being the number density, $\boldsymbol{V}^k$ the velocity (including drift and diffusion), and W_k the chemical source terms (due to Townsend ionization, dissociative recombination, etc) of the kth species. When the plasma is weakly-ionized, it can be shown [16] that the momentum equation collapses to:

$$\boldsymbol{V}_i^k = \boldsymbol{V}_i^{\mathrm{n}} + s_k \mu_k \boldsymbol{E}_i - \frac{\mu_k}{|C_k| N_k} \frac{\partial \boldsymbol{P}_k}{\partial x_i} \tag{2}$$

with $\boldsymbol{V}^{\mathrm{n}}$ the neutrals velocity and with s_k the sign of the charge ($+1$ for positive ions and -1 for negative ions and electrons), μ_k the mobility, C_k the charge ($-e$ for electrons, $+e$ for singly-charged positive ions, $-2e$ for doubly-charged negative ions, etc, with e the elementary charge). Equation (2) depends on the partial pressure P_k which can be found from the density and the temperature using the ideal gas law:

$$P_k = N_k k_{\mathrm{B}} T_k \tag{3}$$

where k_{B} is the Boltzmann constant and T_k is the temperature of species k. As well, Eq. (2) depends on the electric field $\boldsymbol{E}$, which can be found from Gauss's law:

$$\sum_{j=1}^{3} \frac{\partial \boldsymbol{E}_j}{\partial x_j} = \frac{1}{\epsilon_0} \sum_{k=1}^{n_{\mathrm{s}}} C_k N_k \tag{4}$$

where ϵ_0 is the permittivity of free space and n_{s} refers to the number of charged species. To close the set of equations, we assume that the curl of the electric field is zero, hence leading to the existence of an electric field potential

$$\boldsymbol{E}_j = -\frac{\partial \phi}{\partial x_j} \tag{5}$$

with ϕ the potential function. The latter holds true as long as the magnetic field is negligible or does not vary in time, which is a fair assumption for many weakly-ionized plasmas in the absence of an externally-applied time-varying magnetic field because the current due to the induced magnetic field is typically orders of magnitude less than the current due to the electric field.

An important physical parameter that needs to be extracted from the physical model is the current density. We can obtain the current density conservation equation by multiplying the kth species transport Eq. (1), by its respective charge C_k, summing over all species, substituting the species velocity from Eq. (2), and noting that no net charge can be created or destroyed through the chemical reactions. Then, the following equation would be obtained [16]:

$$\frac{\partial \rho_\mathrm{e}}{\partial t} + \sum_{i=1}^{3} \frac{\partial \boldsymbol{J}_i}{\partial x_i} = 0 \tag{6}$$

where the conductivity, the net charge density, and the current density due to drift and diffusion are defined as:

$$\sigma \equiv \sum_{k=1}^{n_\mathrm{s}} |C_k| N_k \mu_k \tag{7}$$

$$\rho_\mathrm{e} \equiv \sum_{k=1}^{n_\mathrm{s}} C_k N_k \tag{8}$$

$$\boldsymbol{J}_i \equiv \sigma \boldsymbol{E}_i - \sum_{k=1}^{n_\mathrm{s}} s_k \mu_k \frac{\partial \boldsymbol{P}_k}{\partial x_i} + \sum_{k=1}^{n_\mathrm{s}} C_k N_k \boldsymbol{V}_i^\mathrm{n} \tag{9}$$

It is emphasized that $\boldsymbol{J}$ is here defined as the current density due to drift and diffusion only, and does not include the displacement current. However, this does not prevent the equations from being used in a situation where the displacement current is significant (such as for a RF discharge for instance). For such a case, the charged densities and the potential are obtained using exactly the same equations as above with $\boldsymbol{J}$ being limited to the current due to drift and diffusion. The displacement current needs to be added to $\boldsymbol{J}$ only when calculating the total current and the phase relations between the applied voltage and the discharge current needed for the external circuit.

The fluid model outlined above is hence valid both in the non-neutral sheaths and the quasi-neutral regions of weakly-ionized plasmas, and can predict accurately physical phenomena such as ambipolar diffusion, ambipolar drift, cathode sheaths, dielectric sheaths, unsteady effects in which the displacement current is significant, etc. Nonetheless, it is noted that the physical model considered herein makes several assumptions: (i) the plasma is not subject to an external magnetic field and the induced magnetic field is assumed negligible, (ii) the drag force due to collisions between charged species is negligible compared to the one originating from collisions between charged species and neutrals, and (iii) the forces due to inertia change are assumed small compared to the forces due to collisions. The mathematical expressions for the latter forces as well as the justification for neglecting them when simulating weakly-ionized plasmas can be found in Ref. [16].

Finally it is cautioned that, because the electric field is obtained from Gauss's law, the physical model outlined in this section can not be used to tackle problems where the electric field is a significant function of a time-varying magnetic field, such as in inductively coupled plasmas or microwave induced plasmas. In those cases, the electric field would cease to be a potential field and would need to be determined through the full or simplified Maxwell equations. More details on when Gauss's law can and can not be used to determine the electric field can be found in Refs. [17, 18].

3. Conventional Governing Equations

In this section, we give a short outline of the set of differential equations that are commonly used to solve the physical model outlined in the previous section using finite-difference methods (which we denote as the "conventional governing equations"). The conventional governing equations correspond to the solution for each charged species (including positive ions, negative ions and electrons) of the transport equation outlined in Eq. (1) with the velocity taken from Eq. (2) and the partial pressure obtained from Eq. (3)

$$\frac{\partial N_k}{\partial t} + \sum_{i=1}^{3} \frac{\partial}{\partial x_i} \left(\boldsymbol{V}_i^\mathrm{n} N_k + s_k \mu_k \boldsymbol{E}_i N_k \right) - \sum_{i=1}^{3} \frac{\partial}{\partial x_i} \left(\frac{\mu_k k_\mathrm{B} T_k}{|C_k|} \frac{\partial N_k}{\partial x_i} \right) = W_k + \sum_{i=1}^{3} \frac{\partial}{\partial x_i} \left(\frac{\mu_k k_\mathrm{B} N_k}{|C_k|} \frac{\partial T_k}{\partial x_i} \right) \tag{10}$$

The electric field appearing in the convection terms is obtained by solving the potential equation based on Gauss's law, which can be obtained by substituting Eq. (5) into Eq. (4):

$$\sum_{j=1}^{3} \frac{\partial^2 \phi}{\partial x_j^2} = -\frac{1}{\epsilon_0} \sum_{k=1}^{n_s} C_k N_k \tag{11}$$

from which the electric field components can be found using Eq. (5).

The transport equations for the charged species can be rewritten in the following matrix form to ease their discretization and integration:

$$R = Z \frac{\partial U}{\partial t} + \sum_{i=1}^{3} \frac{\partial}{\partial x_i}(A_i U) - \sum_{i=1}^{3} \frac{\partial}{\partial x_i}\left(K \frac{\partial U}{\partial x_i}\right) - S \tag{12}$$

where R is the residual vector that we seek to minimize and where the other matrices correspond to:

$$U = \begin{bmatrix} N_1 \\ \vdots \\ N_{n_s} \end{bmatrix} \quad A_i = \begin{bmatrix} \boldsymbol{V}_i^{\mathrm{n}} + s_1 \mu_1 \boldsymbol{E}_i \\ \vdots \\ \boldsymbol{V}_i^{\mathrm{n}} + s_{n_s} \mu_{n_s} \boldsymbol{E}_i \end{bmatrix}^{\mathrm{D}} \quad Z = \begin{bmatrix} 1 \\ \vdots \\ 1 \end{bmatrix}^{\mathrm{D}} \tag{13}$$

$$K = \begin{bmatrix} \dfrac{\mu_1 k_{\mathrm{B}} T_1}{|C_1|} \\ \vdots \\ \dfrac{\mu_{n_s} k_{\mathrm{B}} T_{n_s}}{|C_{n_s}|} \end{bmatrix}^{\mathrm{D}} \quad S = \begin{bmatrix} W_1 + \displaystyle\sum_{i=1}^{3} \frac{\partial}{\partial x_i}\left(\frac{\mu_1 k_{\mathrm{B}} N_1}{|C_1|} \frac{\partial T_1}{\partial x_i}\right) \\ \vdots \\ W_{n_s} + \displaystyle\sum_{i=1}^{3} \frac{\partial}{\partial x_i}\left(\frac{\mu_{n_s} k_{\mathrm{B}} N_{n_s}}{|C_{n_s}|} \frac{\partial T_{n_s}}{\partial x_i}\right) \end{bmatrix} \tag{14}$$

When discretized using finite difference stencils, the set of equations presented in this section and denoted as "conventional" is well-known to be particularly stiff within quasi-neutral regions. This is attributed to the potential equation based on Gauss's law being overly sensitive to small errors in the charged species densities when the plasma becomes quasi-neutral [6]. This makes it necessary to limit the time step to very small values when integrating the electron and ion transport equations, resulting in hundreds of thousands of iterations necessary to reach steady-state.

4. Recast of the Electron and Ion Transport Equations

As was demonstrated in Refs. [7, 6], the stiffness of the system can be alleviated by rewriting the equations such that the electric field potential is not obtained from Gauss's law, but rather from Ohm's law. In so-doing, the potential equation is not overly sensitive to small errors in the densities, and the computational effort can be reduced one hundred fold or even more. The methods presented in Refs. [7] and [6] are however not directly applicable to multidimensional multicomponent plasmas. In this section, we propose a new set of transport equations for the charged species that, when solved in conjunction with a potential equation based on Ohm's law, yields the same answer as the conventional governing equations outlined in Section 3 while requiring a fraction of the computational effort for plasmas involving quasi-neutral regions.

4.1. Positively-Charged Species

When the electric field is obtained from Ohm's law rather than from Gauss's law, it is necessary to add some source terms to the positive ion transport equations to ensure that Gauss's law is satisfied. This can be accomplished as follows. First, substitute the velocity in Eq. (2) into Eq. (1), and simplify noting that $s_k = 1$ and C_k is positive for the positive ions:

$$\frac{\partial N_k}{\partial t} + \sum_{i=1}^{3} \frac{\partial}{\partial x_i}\left(N_k \boldsymbol{V}_i^{\mathrm{n}} + N_k \mu_k \boldsymbol{E}_i - \frac{\mu_k}{|C_k|} \frac{\partial P_k}{\partial x_i}\right) = W_k \tag{15}$$

The source terms that must be added to ensure that Gauss's law is satisfied can be obtained by multiplying Gauss's law Eq. (4) by $\mu_k N_k$ and rearranging:

$$0 = \mu_k N_k \sum_{i=1}^{3} \frac{\partial \boldsymbol{E}_i}{\partial x_i} - \mu_k N_k \frac{1}{\epsilon_0} \sum_{r=1}^{n_s} C_r N_r \tag{16}$$

Then, we add the latter to the former to obtain:

$$\frac{\partial N_k}{\partial t} + \sum_{i=1}^{3} \frac{\partial}{\partial x_i} \left(N_k \boldsymbol{V}_i^{\mathrm{n}} + N_k \mu_k \boldsymbol{E}_i - \frac{\mu_k}{|C_k|} \frac{\partial P_k}{\partial x_i} \right) = W_k + \mu_k N_k \sum_{i=1}^{3} \frac{\partial \boldsymbol{E}_i}{\partial x_i} - \mu_k N_k \frac{1}{\epsilon_0} \sum_{r=1}^{n_\mathrm{s}} C_r N_r \tag{17}$$

And we note that the following statement holds:

$$\mu_k N_k \sum_{i=1}^{3} \frac{\partial \boldsymbol{E}_i}{\partial x_i} = \sum_{i=1}^{3} \frac{\partial}{\partial x_i} \left(\mu_k N_k \boldsymbol{E}_i \right) - \sum_{i=1}^{3} \boldsymbol{E}_i \frac{\partial}{\partial x_i} (\mu_k N_k) \tag{18}$$

Substitute the latter in the former and rearrange:

$$\frac{\partial N_k}{\partial t} + \sum_{i=1}^{3} \frac{\partial}{\partial x_i} \left(N_k \boldsymbol{V}_i^{\mathrm{n}} - \frac{\mu_k}{|C_k|} \frac{\partial P_k}{\partial x_i} \right) + \sum_{i=1}^{3} \boldsymbol{E}_i \frac{\partial}{\partial x_i} (\mu_k N_k) = W_k - \mu_k N_k \frac{1}{\epsilon_0} \sum_{r=1}^{n_\mathrm{s}} C_r N_r \tag{19}$$

Rewrite the partial pressure term using the ideal gas law $P_k = N_k k_\mathrm{B} T_k$, expand the pressure derivatives, and rearrange:

$$\begin{aligned} &\frac{\partial N_k}{\partial t} + \sum_{i=1}^{3} \frac{\partial}{\partial x_i} \left(N_k \boldsymbol{V}_i^{\mathrm{n}} \right) - \sum_{i=1}^{3} \frac{\partial}{\partial x_i} \left(\frac{\mu_k k_\mathrm{B} T_k}{|C_k|} \frac{\partial N_k}{\partial x_i} \right) + \sum_{i=1}^{3} \boldsymbol{E}_i \frac{\partial}{\partial x_i} (\mu_k N_k) \\ &\quad = W_k - \mu_k N_k \frac{1}{\epsilon_0} \sum_{r=1}^{n_\mathrm{s}} C_r N_r + \sum_{i=1}^{3} \frac{\partial}{\partial x_i} \left(\frac{\mu_k k_\mathrm{B} N_k}{|C_k|} \frac{\partial T_k}{\partial x_i} \right) \end{aligned} \tag{20}$$

The latter is the proposed transport equation for the positive ions. It differs from the standard form (Eq. (1)) by including some source terms to ensure that Gauss's law is satisfied when the equations are integrated along with a potential equation based on Ohm's law. However, this modification to the transport equations reduces their resolution capabilities with the consequence that significantly more nodes are needed to capture sheaths and quasi-neutral regions.

4.2. Negatively-Charged Species

One approach that has been shown successful in increasing the resolution of the system of equations is to rewrite the electron transport equation in "ambipolar form" [6]. A transport equation can be written in "ambipolar form" by extracting from the convection terms the ambipolar diffusion terms [19]. Effectively, this increases the computational efficiency when integrating the system because the transport equations for the charged species do not depend as much on the potential. It is here found necessary to rewrite in ambipolar form not only the electron transport equation, but also the transport equations for the negative ions. In doing so, the proposed system of equations (in which the potential is obtained from Ohm's law) exhibits a resolution as high (or even exceeding) the one of the conventional set of equations in which the potential is obtained from Gauss's law.

The ambipolar form outlined herein differs from the one outlined in Ref. [19] by being applicable to a non-neutral plasma and from the one outlined in Ref. [6] by being applicable to a multicomponent plasma. As well, the recast proposed in this section fixes a major problem that was encountered with the ambipolar form in a previous paper: that is, the method proposed herein can be integrated successfully within the negatively-charged plasma region near the anode without requiring a rewrite of the anode boundary conditions. This is here accomplished by defining slightly differently the so-called "ambipolar electric field". In the previous papers, the ambipolar electric field was defined as the component of the electric field that is responsible for cancelling out the component of the current originating from the mass diffusion of the charged species. In this paper, we rather define the ambipolar electric field as the component of the electric field that cancels out all components of the current except due to drift:

$$\boldsymbol{E}_i' \equiv \boldsymbol{E}_i - \frac{1}{\sigma} \boldsymbol{J}_i \tag{21}$$

After substituting the current from Eq. (9) and using the ideal gas law $P_r = N_r k_\mathrm{B} T_r$, it can be shown that:

$$\boldsymbol{E}_i' = \sum_{r=1}^{n_\mathrm{s}} \frac{s_r \mu_r k_\mathrm{B} T_r}{\sigma} \frac{\partial N_r}{\partial x_i} + \sum_{r=1}^{n_\mathrm{s}} \frac{s_r \mu_r k_\mathrm{B} N_r}{\sigma} \frac{\partial T_r}{\partial x_i} - \sum_{r=1}^{n_\mathrm{s}} \frac{C_r N_r}{\sigma} \boldsymbol{V}_i^{\mathrm{n}} \tag{22}$$

where k_B is the Boltzmann constant and T_r is the temperature of species r. Having defined the ambipolar electric field, we now proceed to recast the negatively-charged species in ambipolar form. This can be done by first substituting the velocity in Eq.

(2) into the species transport equation Eq. (1) while noting that $s_k = -1$ when the species is negatively-charged:

$$\frac{\partial N_k}{\partial t} + \sum_{i=1}^{3} \frac{\partial}{\partial x_i} N_k \left(\boldsymbol{V}_i^{\mathrm{n}} - \mu_k \boldsymbol{E}_i - \frac{\mu_k}{|C_k| N_k} \frac{\partial P_k}{\partial x_i} \right) = W_k \tag{23}$$

Then we use the relationship $P_k = N_k k_{\mathrm{B}} T_k$, expand the partial derivatives, and rewrite:

$$\frac{\partial N_k}{\partial t} + \sum_{i=1}^{3} \frac{\partial}{\partial x_i} \left(N_k \boldsymbol{V}_i^{\mathrm{n}} - \mu_k N_k \boldsymbol{E}_i \right) - \sum_{i=1}^{3} \frac{\partial}{\partial x_i} \left(\frac{\mu_k k_{\mathrm{B}} T_k}{|C_k|} \frac{\partial N_k}{\partial x_i} \right) = W_k + \sum_{i=1}^{3} \frac{\partial}{\partial x_i} \left(\frac{\mu_k k_{\mathrm{B}} N_k}{|C_k|} \frac{\partial T_k}{\partial x_i} \right) \tag{24}$$

The latter can be recast in ambipolar form without loss of generality by adding and subtracting $\boldsymbol{E}'$ to the electric field:

$$\begin{aligned} &\frac{\partial N_k}{\partial t} + \sum_{i=1}^{3} \frac{\partial}{\partial x_i} \left(N_k \boldsymbol{V}_i^{\mathrm{n}} - \mu_k N_k \left(\boldsymbol{E} - \boldsymbol{E}' \right)_i \right) - \sum_{i=1}^{3} \frac{\partial}{\partial x_i} \mu_k N_k \boldsymbol{E}_i' \\ &\quad - \sum_{i=1}^{3} \frac{\partial}{\partial x_i} \left(\frac{\mu_k k_{\mathrm{B}} T_k}{|C_k|} \frac{\partial N_k}{\partial x_i} \right) = W_k + \sum_{i=1}^{3} \frac{\partial}{\partial x_i} \left(\frac{\mu_k k_{\mathrm{B}} N_k}{|C_k|} \frac{\partial T_k}{\partial x_i} \right) \end{aligned} \tag{25}$$

After substituting $\boldsymbol{E}'$ from Eq. (22) in the third term on the LHS and rearranging, we obtain:

$$\begin{aligned} &\frac{\partial N_k}{\partial t} + \sum_{i=1}^{3} \frac{\partial}{\partial x_i} \left(N_k \boldsymbol{V}_i^{\mathrm{n}} - \mu_k N_k \left(\boldsymbol{E} - \boldsymbol{E}' \right)_i \right) - \sum_{i=1}^{3} \frac{\partial}{\partial x_i} \left(\mu_k N_k \sum_{r=1}^{n_{\mathrm{s}}} \frac{s_r \mu_r k_{\mathrm{B}} T_r}{\sigma} \frac{\partial N_r}{\partial x_i} \right) - \sum_{i=1}^{3} \frac{\partial}{\partial x_i} \left(\frac{\mu_k k_{\mathrm{B}} T_k}{|C_k|} \frac{\partial N_k}{\partial x_i} \right) \\ &\quad = W_k + \sum_{i=1}^{3} \frac{\partial}{\partial x_i} \left(\frac{\mu_k k_{\mathrm{B}} N_k}{|C_k|} \frac{\partial T_k}{\partial x_i} \right) + \sum_{i=1}^{3} \frac{\partial}{\partial x_i} \left(\mu_k N_k \sum_{r=1}^{n_{\mathrm{s}}} \frac{s_r \mu_r k_{\mathrm{B}} N_r}{\sigma} \frac{\partial T_r}{\partial x_i} \right) - \sum_{i=1}^{3} \frac{\partial}{\partial x_i} \left(\mu_k N_k \sum_{r=1}^{n_{\mathrm{s}}} \frac{C_r N_r}{\sigma} \boldsymbol{V}_i^{\mathrm{n}} \right) \end{aligned} \tag{26}$$

Split the second-last term on the LHS in two and simplify:

$$\begin{aligned} &\frac{\partial N_k}{\partial t} + \sum_{i=1}^{3} \frac{\partial}{\partial x_i} \left(N_k \boldsymbol{V}_i^{\mathrm{n}} - \mu_k N_k \left(\boldsymbol{E} - \boldsymbol{E}' \right)_i \right) - \sum_{i=1}^{3} \frac{\partial}{\partial x_i} \left(\mu_k N_k \sum_{r=1..n_{\mathrm{s}}}^{r \neq k} \frac{s_r \mu_r k_{\mathrm{B}} T_r}{\sigma} \frac{\partial N_r}{\partial x_i} \right) \\ &\quad + \sum_{i=1}^{3} \frac{\partial}{\partial x_i} \left(\frac{\mu_k^2 N_k k_{\mathrm{B}} T_k}{\sigma} \frac{\partial N_k}{\partial x_i} \right) - \sum_{i=1}^{3} \frac{\partial}{\partial x_i} \left(\frac{\mu_k k_{\mathrm{B}} T_k}{|C_k|} \frac{\partial N_k}{\partial x_i} \right) = W_k + \sum_{i=1}^{3} \frac{\partial}{\partial x_i} \left(\frac{\mu_k k_{\mathrm{B}} N_k}{|C_k|} \frac{\partial T_k}{\partial x_i} \right) \\ &\quad + \sum_{i=1}^{3} \frac{\partial}{\partial x_i} \left(\mu_k N_k \sum_{r=1}^{n_{\mathrm{s}}} \frac{s_r \mu_r k_{\mathrm{B}} N_r}{\sigma} \frac{\partial T_r}{\partial x_i} \right) - \sum_{i=1}^{3} \frac{\partial}{\partial x_i} \left(\mu_k N_k \sum_{r=1}^{n_{\mathrm{s}}} \frac{C_r N_r}{\sigma} \boldsymbol{V}_i^{\mathrm{n}} \right) \end{aligned} \tag{27}$$

Combine the last 2 terms on the LHS:

$$\begin{aligned} &\frac{\partial N_k}{\partial t} + \sum_{i=1}^{3} \frac{\partial}{\partial x_i} \left(N_k \boldsymbol{V}_i^{\mathrm{n}} - \mu_k N_k \left(\boldsymbol{E} - \boldsymbol{E}' \right)_i \right) - \sum_{i=1}^{3} \sum_{r=1..n_{\mathrm{s}}}^{r \neq k} \frac{\partial}{\partial x_i} \left(\frac{\mu_k N_k s_r \mu_r k_{\mathrm{B}} T_r}{\sigma} \frac{\partial N_r}{\partial x_i} \right) \\ &\quad - \sum_{i=1}^{3} \frac{\partial}{\partial x_i} \left(\frac{\sigma - |C_k| \mu_k N_k}{\sigma |C_k|} \mu_k k_{\mathrm{B}} T_k \frac{\partial N_k}{\partial x_i} \right) = W_k + \sum_{i=1}^{3} \frac{\partial}{\partial x_i} \left(\frac{\mu_k k_{\mathrm{B}} N_k}{|C_k|} \frac{\partial T_k}{\partial x_i} \right) \\ &\quad + \sum_{i=1}^{3} \frac{\partial}{\partial x_i} \left(\mu_k N_k \sum_{r=1}^{n_{\mathrm{s}}} \frac{s_r \mu_r k_{\mathrm{B}} N_r}{\sigma} \frac{\partial T_r}{\partial x_i} \right) - \sum_{i=1}^{3} \frac{\partial}{\partial x_i} \left(\mu_k N_k \sum_{r=1}^{n_{\mathrm{s}}} \frac{C_r N_r}{\sigma} \boldsymbol{V}_i^{\mathrm{n}} \right) \end{aligned} \tag{28}$$

But recall from Eq. (21) that $\boldsymbol{E}_i - \boldsymbol{E}_i' = \boldsymbol{J}_i / \sigma$. After substituting the latter in the above and splitting the derivative involving the current into two terms, we obtain:

$$\begin{aligned} &\frac{\partial N_k}{\partial t} + \sum_{i=1}^{3} \frac{\partial}{\partial x_i} \left(N_k \boldsymbol{V}_i^{\mathrm{n}} \right) - \frac{\mu_k N_k}{\sigma} \sum_{i=1}^{3} \frac{\partial \boldsymbol{J}_i}{\partial x_i} - \sum_{i=1}^{3} \boldsymbol{J}_i \frac{\partial}{\partial x_i} \left(\frac{\mu_k N_k}{\sigma} \right) - \sum_{i=1}^{3} \sum_{r=1..n_{\mathrm{s}}}^{r \neq k} \frac{\partial}{\partial x_i} \left(\frac{\mu_k N_k s_r \mu_r k_{\mathrm{B}} T_r}{\sigma} \frac{\partial N_r}{\partial x_i} \right) \\ &\quad - \sum_{i=1}^{3} \frac{\partial}{\partial x_i} \left(\frac{\sigma - |C_k| \mu_k N_k}{\sigma |C_k|} \mu_k k_{\mathrm{B}} T_k \frac{\partial N_k}{\partial x_i} \right) = W_k + \sum_{i=1}^{3} \frac{\partial}{\partial x_i} \left(\frac{\mu_k k_{\mathrm{B}} N_k}{|C_k|} \frac{\partial T_k}{\partial x_i} \right) \\ &\quad + \sum_{i=1}^{3} \frac{\partial}{\partial x_i} \left(\mu_k N_k \sum_{r=1}^{n_{\mathrm{s}}} \frac{s_r \mu_r k_{\mathrm{B}} N_r}{\sigma} \frac{\partial T_r}{\partial x_i} \right) - \sum_{i=1}^{3} \frac{\partial}{\partial x_i} \left(\mu_k N_k \sum_{r=1}^{n_{\mathrm{s}}} \frac{C_r N_r}{\sigma} \boldsymbol{V}_i^{\mathrm{n}} \right) \end{aligned} \tag{29}$$

But note that, after substituting Eq. (8) into Eq. (6), the divergence of the current can be written as:

$$\sum_{i=1}^{3} \frac{\partial \boldsymbol{J}_i}{\partial x_i} = -\sum_{r=1}^{n_s} C_r \frac{\partial N_r}{\partial t} \tag{30}$$

Then, after substituting the latter in the former and regrouping similar terms together, the following is obtained:

$$\begin{aligned}
&\frac{\sigma - |C_k|\mu_k N_k}{\sigma}\frac{\partial N_k}{\partial t} + \sum_{r=1..n_s}^{r\neq k} \frac{C_r \mu_k N_k}{\sigma}\frac{\partial N_r}{\partial t} + \sum_{i=1}^{3}\frac{\partial}{\partial x_i}\left(N_k \boldsymbol{V}_i^{\mathrm{n}}\right) - \sum_{i=1}^{3} \boldsymbol{J}_i \frac{\partial}{\partial x_i}\left(\frac{\mu_k N_k}{\sigma}\right) \\
&- \sum_{i=1}^{3}\sum_{r=1..n_s}^{r\neq k} \frac{\partial}{\partial x_i}\left(\frac{\mu_k N_k s_r \mu_r k_{\mathrm{B}} T_r}{\sigma}\frac{\partial N_r}{\partial x_i}\right) - \sum_{i=1}^{3}\frac{\partial}{\partial x_i}\left(\frac{\sigma - |C_k|\mu_k N_k}{\sigma |C_k|}\mu_k k_{\mathrm{B}} T_k \frac{\partial N_k}{\partial x_i}\right) = W_k \\
&+ \sum_{i=1}^{3}\frac{\partial}{\partial x_i}\left(\frac{\mu_k k_{\mathrm{B}} N_k}{|C_k|}\frac{\partial T_k}{\partial x_i}\right) + \sum_{i=1}^{3}\frac{\partial}{\partial x_i}\left(\mu_k N_k \sum_{r=1}^{n_s}\frac{s_r \mu_r k_{\mathrm{B}} N_r}{\sigma}\frac{\partial T_r}{\partial x_i}\right) - \sum_{i=1}^{3}\frac{\partial}{\partial x_i}\left(\mu_k N_k \sum_{r=1}^{n_s}\frac{C_r N_r}{\sigma}\boldsymbol{V}_i^{\mathrm{n}}\right)
\end{aligned} \tag{31}$$

The latter is the proposed "ambipolar form" of the transport equation for the negatively-charged species. It must be used not only for the electrons but for all negative ions. It is emphasized that the recast Eq. (31) is obtained from the physical model outlined in Section 2 without making any assumption.

5. Proposed Governing Equations

We can combine the transport equation for the positively-charged species, Eq. (20) and the transport equation for the negatively-charged species, Eq. (31) into a single equation:

$$\begin{aligned}
&\frac{\sigma - \beta_k^- |C_k|\mu_k N_k}{\sigma}\frac{\partial N_k}{\partial t} + \sum_{r=1..n_s}^{r\neq k} \frac{\beta_k^- C_r \mu_k N_k}{\sigma}\frac{\partial N_r}{\partial t} + \sum_{i=1}^{3}\frac{\partial}{\partial x_i}\left(\boldsymbol{V}_i^{\mathrm{n}} N_k\right) + \sum_{i=1}^{3}\frac{\partial}{\partial x_i}\left(\beta_k^- \mu_k \sum_{r=1}^{n_s}\frac{C_r N_r}{\sigma}\boldsymbol{V}_i^{\mathrm{n}} N_k\right) \\
&- \sum_{i=1}^{3}\sum_{r=1..n_s}^{r\neq k} \frac{\partial}{\partial x_i}\left(\frac{\beta_k^- \mu_k N_k s_r \mu_r k_{\mathrm{B}} T_r}{\sigma}\frac{\partial N_r}{\partial x_i}\right) - \sum_{i=1}^{3}\frac{\partial}{\partial x_i}\left(\frac{\sigma - \beta_k^- |C_k|\mu_k N_k}{\sigma |C_k|}\mu_k k_{\mathrm{B}} T_k \frac{\partial N_k}{\partial x_i}\right) \\
&- \sum_{i=1}^{3}\beta_k^- \boldsymbol{J}_i \frac{\partial}{\partial x_i}\left(\frac{\mu_k N_k}{\sigma}\right) + \sum_{i=1}^{3}\beta_k^+ \boldsymbol{E}_i \frac{\partial}{\partial x_i}(\mu_k N_k) = W_k - \beta_k^+ \mu_k N_k \frac{1}{\epsilon_0}\sum_{r=1}^{n_s} C_r N_r \\
&+ \sum_{i=1}^{3}\frac{\partial}{\partial x_i}\left(\frac{\mu_k k_{\mathrm{B}} N_k}{|C_k|}\frac{\partial T_k}{\partial x_i}\right) + \sum_{i=1}^{3}\frac{\partial}{\partial x_i}\left(\beta_k^- \mu_k N_k \sum_{r=1}^{n_s}\frac{s_r \mu_r k_{\mathrm{B}} N_r}{\sigma}\frac{\partial T_r}{\partial x_i}\right)
\end{aligned} \tag{32}$$

where $\beta^+ = 1$ and $\beta^- = 0$ for the positively-charged species and $\beta^+ = 0$ and $\beta^- = 1$ for the negatively-charged species. We can express $\beta^\pm$ in a single expression as follows:

$$\beta_k^\pm = \max(0,\ \pm s_k) \tag{33}$$

The current density is obtained from Eq. (9) while the electric field is obtained from the potential equation based on Ohm's law. The potential based on Ohm's law can be obtained by substituting Eqs. (5), (9) and (8) in the current continuity (Eq. (6)) and rearranging:

$$\sum_{i=1}^{3}\frac{\partial}{\partial x_i}\left(-\sigma\frac{\partial \phi}{\partial x_i}\right) = -\frac{\partial \rho_{\mathrm{e}}}{\partial t} + \sum_{i=1}^{3}\frac{\partial}{\partial x_i}\left(\sum_{k=1}^{n_s} s_k \mu_k \frac{\partial P_k}{\partial x_i} - \rho_{\mathrm{e}}\boldsymbol{V}_i^{\mathrm{n}}\right) \tag{34}$$

To simplify the discretization and integration processes, it is convenient to rewrite Eq. (32) in general matrix form as follows:

$$R = Z\frac{\partial U}{\partial t} + \sum_{i=1}^{3}\frac{\partial}{\partial x_i}(A_i U) + \sum_{i=1}^{3} G_i \frac{\partial}{\partial x_i}(BU) - \sum_{i=1}^{3}\frac{\partial}{\partial x_i}\left(K\frac{\partial U}{\partial x_i}\right) - S \tag{35}$$

where R is the residual vector that we seek to minimize and where the other matrices correspond to:

$$U = \begin{bmatrix} N_1 \\ \vdots \\ N_{n_s} \end{bmatrix} \quad A_i = \begin{bmatrix} \boldsymbol{V}_i^{\mathrm{n}} + \frac{1}{\sigma}\beta_1^- \mu_1 \rho_{\mathrm{e}} \boldsymbol{V}_i^{\mathrm{n}} \\ \vdots \\ \boldsymbol{V}_i^{\mathrm{n}} + \frac{1}{\sigma}\beta_{n_s}^- \mu_{n_s} \rho_{\mathrm{e}} \boldsymbol{V}_i^{\mathrm{n}} \end{bmatrix}^{\mathrm{D}} \quad B = \begin{bmatrix} \beta_1^+ \mu_1 + \frac{1}{\sigma}\beta_1^- \mu_1 \\ \vdots \\ \beta_{n_s}^+ \mu_{n_s} + \frac{1}{\sigma}\beta_{n_s}^- \mu_{n_s} \end{bmatrix}^{\mathrm{D}} \quad G_i = \begin{bmatrix} \beta_1^+ \boldsymbol{E}_i - \beta_1^- \boldsymbol{J}_i \\ \vdots \\ \beta_{n_s}^+ \boldsymbol{E}_i - \beta_{n_s}^- \boldsymbol{J}_i \end{bmatrix}^{\mathrm{D}} \tag{36}$$

$$K = \begin{bmatrix} [K]_{1,1} & \cdots & [K]_{1,n_s} \\ \vdots & \ddots & \vdots \\ [K]_{n_s,1} & \cdots & [K]_{n_s,n_s} \end{bmatrix} \quad \text{with} \quad [K]_{r,k} = \begin{cases} \dfrac{\sigma - \beta_r^- \mu_r |C_r| N_r}{\sigma |C_r|} \mu_r k_B T_r & \text{if } r = k \\ \dfrac{\beta_r^- \mu_r N_r s_k \mu_k k_B T_k}{\sigma} & \text{otherwise} \end{cases} \tag{37}$$

$$Z = \begin{bmatrix} [Z]_{1,1} & \cdots & [Z]_{1,n_s} \\ \vdots & \ddots & \vdots \\ [Z]_{n_s,1} & \cdots & [Z]_{n_s,n_s} \end{bmatrix} \quad \text{with} \quad [Z]_{r,k} = \begin{cases} \dfrac{\sigma - \beta_r^- |C_r| \mu_r N_r}{\sigma} & \text{if } r = k \\ \dfrac{\beta_r^- C_k \mu_r N_r}{\sigma} & \text{otherwise} \end{cases} \tag{38}$$

$$S = \begin{bmatrix} W_1 - \beta_1^+ \mu_1 N_1 \dfrac{\rho_e}{\epsilon_0} + \displaystyle\sum_{i=1}^{3} \frac{\partial}{\partial x_i} \left(\frac{\mu_1 k_B N_1}{|C_1|} \frac{\partial T_1}{\partial x_i} \right) + \sum_{i=1}^{3} \frac{\partial}{\partial x_i} \left(\beta_1^- \mu_1 N_1 \displaystyle\sum_{r=1}^{n_s} \frac{s_r \mu_r k_B N_r}{\sigma} \frac{\partial T_r}{\partial x_i} \right) \\ \vdots \\ W_{n_s} - \beta_{n_s}^+ \mu_{n_s} N_{n_s} \dfrac{\rho_e}{\epsilon_0} + \displaystyle\sum_{i=1}^{3} \frac{\partial}{\partial x_i} \left(\frac{\mu_{n_s} k_B N_{n_s}}{|C_{n_s}|} \frac{\partial T_{n_s}}{\partial x_i} \right) + \sum_{i=1}^{3} \frac{\partial}{\partial x_i} \left(\beta_{n_s}^- \mu_{n_s} N_{n_s} \displaystyle\sum_{r=1}^{n_s} \frac{s_r \mu_r k_B N_r}{\sigma} \frac{\partial T_r}{\partial x_i} \right) \end{bmatrix} \tag{39}$$

It is emphasized that the transport equations proposed in Eq. (35) along with the potential equation based on Ohm's law outlined in Eq. (34) are obtained from the physical model outlined in Section 2 *without introducing new assumptions or simplifications*. As such, they always guarantee that Gauss's law is satisfied and yield the same solution as the conventional governing equations shown previously in Section 3, in which the potential equation is based on Gauss's law (see proof in the Appendix demonstrating how the proposed set of equations ensures the solution of Gauss's law). This is true not only for steady-state cases but also for unsteady cases in which the displacement current becomes significant such as when simulating RF discharges for instance (see discussion on this point just below Eq. (9)). However, because the potential equation is based on Ohm's law instead of Gauss's law, the proposed set of governing equations is advantaged by being easier to integrate in plasma regions that are quasi-neutral. As will be shown in the Test Cases section below, this results in a fourtyfold (or more) reduction in computational effort for some typical flowfields, while not compromising on the accuracy of the converged solution.

6. Boundary Conditions

The set of governing equations based on Ohm's law proposed in this paper can be used with the same boundary conditions normally used when solving the conventional set of equations based on Gauss's law. For this purpose, it is convenient to define η as a coordinate that is perpendicular to the boundary surface and that points away from the surface. Then, when the electric field points towards the surface (or when the surface is a dielectric) the electron and ion number densities are set at the surface as follows:

$$\frac{\partial (N_+ V_+)}{\partial \eta} = 0 \quad \text{and} \quad N_- = 0 \quad \text{and} \quad N_e = \frac{\gamma}{\mu_e} \sum_{k=1}^{n_s} N_k \mu_k \beta_k^+ \quad \text{for} \quad \boldsymbol{E}_\eta < 0 \tag{40}$$

with γ being the secondary emission coefficient, the subscript "e" denoting the electron species, the subscript "$-$" denoting the negative ion species, and the subscript "$+$" denoting the positive ion species. On the other hand, when the electric field points away from the surface, the following boundary conditions are imposed on the charged species densities:

$$N_+ = 0 \quad \text{and} \quad \frac{\partial (N_- V_-)}{\partial \eta} = 0 \quad \text{and} \quad \frac{\partial (N_e V_e)}{\partial \eta} = 0 \quad \text{for} \quad \boldsymbol{E}_\eta > 0 \tag{41}$$

When the surface is an electrode, the potential is fixed to a user-defined value. When the surface is a dielectric, the potential must be such that the current perpendicular to the dielectric is zero. A boundary condition for the potential on a dielectric surface can thus be obtained by first setting the current in Eq. (9) to zero and then noting that $\boldsymbol{E}_\eta = -\partial \phi / \partial \eta$:

$$\frac{\partial \phi}{\partial \eta} = -\frac{1}{\sigma} \sum_{k=1}^{n_s} s_k \mu_k \frac{\partial P_k}{\partial \eta} \tag{42}$$

For certain flowfields, it may be necessary to underrelax the change of the electron density at the boundary and to determine the electric field $\boldsymbol{E}_\eta$ using the minmod of the electric fields at the two interfaces closest to the boundary (as done in Ref. [6]). However, contrarily to the approach shown in Ref. [6], it is not necessary to modify the boundary conditions at the anode in

order to ensure that Gauss's law is satisfied within the anode sheath. Rather, we here use the same boundary conditions for the proposed governing equations (in which the potential is obtained from Ohm's law) as for the conventional governing equations (in which the potential is obtained from Gauss's law). This is attributed to an additional transformation of the equations, introduced between Eq. (29) and Eq. (31): because of the different definition of the ambipolar electric field, some spatial derivatives within the negatively-charged species transport equations can be recast in the form of a temporal derivative by using the current continuity equation. This additional transformation reduces the dependence of the transport equations on the electric field, resulting in a higher resolution within the anode sheath.

7. Discretization and Integration

The discretization of the potential equation (see Eq. (34)) does not pose any particular problem and is here accomplished using centered second-order accurate stencils for the spatial derivatives and using first-order backward stencils for the time derivatives. The potential equation is advanced in pseudotime using an approximate factorization implicit algorithm as outlined in Refs. [16, 19], with the pseudotime step being fixed to a constant for all nodes. That is, the pseudotime step for all nodes is fixed to the minimum throughout the domain found from:

$$\Delta\tau_\phi = \begin{cases} L_c \cdot \min\limits_{i=1}^{3} \left(\dfrac{\Delta x_i}{\sigma_{ref} + \sigma} \right) & \text{for the potential based on Ohm's law} \\ L_c \cdot \min\limits_{i=1}^{3} \left(\Delta x_i \right) & \text{for the potential based on Gauss's law} \end{cases} \tag{43}$$

with σ_{ref} a user-defined constant typically set to 0.003 S/m and L_c a characteristic length that is varied depending on the problem (typically set to some average distance between the electrodes). It is found that faster convergence can be attained when varying the characteristic length L_c cyclically from iteration to iteration, such as $L_c = 1, 0.1, 10, 1, 0.1$ m, etc. Exactly how L_c is varied will be specified case by case in the Test Cases section below.

The discretization of the charged species transport equations (see Eq. (35)) is accomplished by splitting the derivatives along each dimension and discretizing the so-obtained one-dimensional derivatives using one-dimensional stencils (i.e. dimensional splitting). The one-dimensional stencils used herein for the various types of derivatives are taken from Ref. [6]. In solving the discretized charged species transport equations, an approximate factorization algorithm is used along with a block-implicit algorithm in which the convection, diffusion and source terms are all linearized and hence treated in an implicit manner. For this purpose, a pseudotime derivative is added to the left-hand-side of the equations. It is noted that the pseudotime step is set to the same value over all nodes, and corresponds to the minimum pseudotime step within the domain found from:

$$\Delta\tau_N = \mathrm{CFL} \cdot \min_{i=1}^{3} \left(\frac{\Delta x_i}{a_{ref} + \mu_e \left| \boldsymbol{E}_i - \boldsymbol{E}'_i \right|} \right) \tag{44}$$

with μ_e the electron mobility, a_{ref} a constant typically set to 300 m/s, and CFL a constant varied from case to case to achieve fastest convergence.

TABLE 1.
3-species 3-reactions air plasma chemical model with electron beam ionization.

No.	Reaction	Rate Coefficient[a]	References
1	$e^- + Air \rightarrow Air^+ + e^- + e^-$	$\exp(-0.0105031 \cdot \ln^2 E^\star - 2.40983 \cdot 10^{-75} \cdot \ln^{46} E^\star)$ cm^3/s	[20, 17, 21][b]
2	$Air \rightarrow e^- + Air^+$	$1.84 \cdot 10^{17} \cdot Q_b^\star$ 1/s	[22]
3	$e^- + Air^+ \rightarrow Air$	$2.24 \cdot 10^{-7} \cdot (300/T_e)^{0.5} + 0.4 \cdot 10^{-7} \cdot (300/T_e)^{0.7}$ cm^3/s	[23][c]

[a] Notation and units: T_e is in Kelvin; T is in Kelvin; $E^\star$ is the reduced electric field ($E^\star \equiv |\boldsymbol{E}|/N$) in units of V·m^2; $Q_b^\star$ is the ratio in Watts between the electron beam power per unit volume Q_b and the total number density of the plasma N ($Q_b^\star \equiv Q_b/N$).

[b] The rate coefficient approximates the Townsend ionization rates given in [20] and in [17, p. 56] with the drift velocity taken from [21, Ch. 21]; The rate coefficient can be used in the range $3 \cdot 10^{-20} \leq E^\star \leq 240 \cdot 10^{-20}$ V · m^2 with a relative error on the ionization rate not exceeding 20%.

[c] The rate coefficient approximates the dissociative recombination reactions $e^- + N_2^+ \rightarrow N + N$ and $e^- + O_2^+ \rightarrow O + O$ assuming a N_2^+:O_2^+ ratio of 4:1.

TABLE 2.
6-species 15-reactions air plasma chemical model with electron beam ionization.[a,b]

No.	Reaction	Rate Coefficient	Refs.
1a	$e^- + N_2 \rightarrow N_2^+ + e^- + e^-$	$\exp(-0.0105809 \cdot \ln^2 E^\star - 2.40411 \cdot 10^{-75} \cdot \ln^{46} E^\star)$ cm^3/s	[21, 20, 17][c]
1b	$e^- + O_2 \rightarrow O_2^+ + e^- + e^-$	$\exp(-0.0102785 \cdot \ln^2 E^\star - 2.42260 \cdot 10^{-75} \cdot \ln^{46} E^\star)$ cm^3/s	[21, 20, 17][c]
2a	$e^- + O_2^+ \rightarrow O_2$	$2.0 \cdot 10^{-7} \cdot (300/T_e)^{0.7}$ cm^3/s	[24][d]
2b	$e^- + N_2^+ \rightarrow N_2$	$2.8 \cdot 10^{-7} \cdot (300/T_e)^{0.5}$ cm^3/s	[23][d]
3a	$O_2^- + N_2^+ \rightarrow O_2 + N_2$	$2.0 \cdot 10^{-7} \cdot (300/T)^{0.5}$ cm^3/s	[23]
3b	$O_2^- + O_2^+ \rightarrow O_2 + O_2$	$2.0 \cdot 10^{-7} \cdot (300/T)^{0.5}$ cm^3/s	[23]
4a	$O_2^- + N_2^+ + N_2 \rightarrow O_2 + N_2 + N_2$	$2.0 \cdot 10^{-25} \cdot (300/T)^{2.5}$ cm^6/s	[23]
4b	$O_2^- + O_2^+ + N_2 \rightarrow O_2 + O_2 + N_2$	$2.0 \cdot 10^{-25} \cdot (300/T)^{2.5}$ cm^6/s	[23]
4c	$O_2^- + N_2^+ + O_2 \rightarrow O_2 + N_2 + O_2$	$2.0 \cdot 10^{-25} \cdot (300/T)^{2.5}$ cm^6/s	[23]
4d	$O_2^- + O_2^+ + O_2 \rightarrow O_2 + O_2 + O_2$	$2.0 \cdot 10^{-25} \cdot (300/T)^{2.5}$ cm^6/s	[23]
5a	$e^- + O_2 + O_2 \rightarrow O_2^- + O_2$	$1.4 \cdot 10^{-29} \cdot (300/T_e) \cdot \exp(-600/T) \cdot \exp\left(\frac{700(T_e-T)}{T_e T}\right)$ cm^6/s	[23]
5b	$e^- + O_2 + N_2 \rightarrow O_2^- + N_2$	$1.07 \cdot 10^{-31} \cdot (300/T_e)^2 \cdot \exp(-70/T) \cdot \exp\left(\frac{1500(T_e-T)}{T_e T}\right)$ cm^6/s	[23]
6	$O_2^- + O_2 \rightarrow e^- + O_2 + O_2$	$8.6 \cdot 10^{-10} \cdot \exp(-6030/T) \cdot (1 - \exp(-1570/T))$ cm^3/s	[25, Ch. 2]
7a	$O_2 \rightarrow e^- + O_2^+$	$2.0 \cdot 10^{17} \cdot Q_b^\star$ 1/s	[26]
7b	$N_2 \rightarrow e^- + N_2^+$	$1.8 \cdot 10^{17} \cdot Q_b^\star$ 1/s	[26]

[a] The species consist of N_2^+, O_2^+, O_2^-, e^-, O_2, N_2.

[b] Notation and units: $E^\star$ is the reduced effective electric field ($E^\star \equiv |\boldsymbol{E}|/N$) in units of V·m^2; T_e is the electron temperature in Kelvin; T is the neutrals temperature in Kelvin; $Q_b^\star$ is the ratio in Watts between the electron beam power per unit volume Q_b and the total number density of the plasma N ($Q_b^\star \equiv Q_b/N$).

[c] The rate coefficient approximates the Townsend ionization rates given in [20] and in [17, p. 56] with the drift velocity taken from [21, Ch. 21]; The rate coefficient for N_2 ionization can be used in the range $3 \cdot 10^{-20} \leq E^\star \leq 187 \cdot 10^{-20}$ V · m^2 with a relative error on the ionization rate not exceeding 17%; The rate coefficient for O_2 ionization is obtained from the rate for air and the one for N_2 assuming a N_2:O_2 ratio of 4:1.

[d] The reaction rates for the dissociative recombination reactions $e^- + O_2^+ \rightarrow O + O$ and $e^- + N_2^+ \rightarrow N + N$ are here rewritten for simplicity to $e^- + O_2^+ \rightarrow O_2$ and $e^- + N_2^+ \rightarrow N_2$ (to avoid the handling of the additional O and N species).

In order to make the pseudotime integration stable it is found necessary not to fully linearize the electron impact ionization (i.e. Townsend ionization) terms. Rather, we here propose a partial linearization of the Townsend ionization terms that is stable and that results in faster convergence. This is accomplished by first rewriting the electron impact source terms as a function of current (instead of electric field), and then linearizing under the condition of quasi-constant current. For this purpose, we can rewrite the reduced electric field as:

$$\frac{|\boldsymbol{E}|}{N} = \frac{|\xi|}{\sigma} \tag{45}$$

After obtaining the electric field as a function of the current from Eq. (9) and substituting, it follows that ξ_i is equal to:

$$\xi_i = \frac{1}{N}\left(\boldsymbol{J}_i + \sum_{k=1}^{n_s} s_k \mu_k \frac{\partial P_k}{\partial x_i} - \sum_{k=1}^{n_s} C_k N_k \boldsymbol{V}_i^n\right) \tag{46}$$

Then note that the electron impact ionization rates can be written as follows (see reaction 1 in Table 1 and reactions 1a and 1b in Table 2):

$$k_{ei} = \exp(-\theta_1 \cdot \ln^2 E^\star - \theta_2 \cdot \ln^{46} E^\star) \tag{47}$$

with θ_1 and θ_2 some constants. Substitute $E^\star = |\boldsymbol{E}|/N = |\xi|/\sigma$ in the latter and take the derivative with respect to σ on both sides keeping ξ constant (a constant ξ essentially entails a constant current density because ξ depends mostly on the current density $\boldsymbol{J}$ within the cathode sheath where the Townsend ionization takes place):

$$\left(\frac{\partial k_{ei}}{\partial \sigma}\right)_\xi = k_{ei}\left(\frac{2\theta_1}{\sigma}\ln E^\star + \frac{46\theta_2}{\sigma}\ln^{45} E^\star\right) \tag{48}$$

But recall that the conductivity is proportional to the number density of each species (Eq. (7)). Assuming constant mobilities, it follows that:

$$\left(\frac{\partial k_{\mathrm{ei}}}{\partial N_k}\right)_\xi = \left(\frac{\partial \sigma}{\partial N_k}\right)_\xi \times \left(\frac{\partial k_{\mathrm{ei}}}{\partial \sigma}\right)_\xi = |C_k|\mu_k k_{\mathrm{ei}}\left(\frac{2\theta_1}{\sigma}\ln E^\star + \frac{46\theta_2}{\sigma}\ln^{45} E^\star\right) \tag{49}$$

For instance, consider a plasma composed of O_2, N_2, N_2^+, O_2^+, O_2^-, and electrons. The Townsend ionization rate k_{1a} for the reaction $e^- + N_2 \rightarrow N_2^+ + e^- + e^-$ can be approximated by Eq. (47) with $\theta_1 = 0.0105809$ and $\theta_2 = 2.40411 \times 10^{-75}$. The U vector in this case would be limited to the charged species and would hence correspond to $U = [N_{O_2^+} \;\; N_{N_2^+} \;\; N_{O_2^-} \;\; N_e]^T$. The contributions to the source term Jacobian $M = \partial S/\partial U$ originating from reaction 1a would then amount to:

$$M_{1a} = \begin{bmatrix} 0 & 0 & 0 & 0 \\ N_{N_2}N_e\left(\frac{\partial k_{1a}}{\partial N_{O_2^+}}\right)_\xi & N_{N_2}N_e\left(\frac{\partial k_{1a}}{\partial N_{N_2^+}}\right)_\xi & N_{N_2}N_e\left(\frac{\partial k_{1a}}{\partial N_{O_2^-}}\right)_\xi & N_{N_2}N_e\left(\frac{\partial k_{1a}}{\partial N_e}\right)_\xi \\ 0 & 0 & 0 & 0 \\ N_{N_2}N_e\left(\frac{\partial k_{1a}}{\partial N_{O_2^+}}\right)_\xi & N_{N_2}N_e\left(\frac{\partial k_{1a}}{\partial N_{N_2^+}}\right)_\xi & N_{N_2}N_e\left(\frac{\partial k_{1a}}{\partial N_{O_2^-}}\right)_\xi & N_{N_2}N_e\left(\frac{\partial k_{1a}}{\partial N_e}\right)_\xi \end{bmatrix} \tag{50}$$

where the various $(\partial k_{1a}/\partial N_k)_\xi$ terms are taken from Eq. (49). The source term Jacobian M includes the contributions from all chemical reactions as well as the contribution from the extra source term added to the positively-charged transport equations to ensure that Gauss's law is satisfied:

$$M = M_g + M_{1a} + M_{1b} + M_{2a} + ... \tag{51}$$

with M_g including only the negative source term needed to enforce Gauss's law:

$$M_g = \begin{bmatrix} [M_g]_{1,1} & \cdots & [M_g]_{1,n_s} \\ \vdots & \ddots & \vdots \\ [M_g]_{n_s,1} & \cdots & [M_g]_{n_s,n_s} \end{bmatrix} \quad \text{with} \quad [M_g]_{r,k} = \begin{cases} -\dfrac{1}{\epsilon_0}\beta_r^+\mu_r \displaystyle\sum_{m=1}^{n_s} \max(0,\, C_m)\, N_m & \text{if } r = k \\ -\dfrac{1}{\epsilon_0}\beta_r^+\mu_r N_r \max(0,\, C_k) & \text{otherwise} \end{cases} \tag{52}$$

It is emphasized that only the electron-impact reactions are linearized as in Eq. (50). The other chemical reactions do not pose any problem and are linearized in the standard manner by taking the partial derivative of the chemical source term with respect to a particular number density (keeping the other number densities constant).

One iteration consists of first advancing in pseudotime in coupled form the transport equations for the number densities while keeping the potential constant. This is followed by 2 or 3 subiterations in pseudotime of the potential equation keeping the number densities constant. The process is repeated as long as the residual of all charged species transport equations and of the potential equation is above some user-specified convergence thresholds. When solving certain sheath problems, it is found necessary to perform some pseudotime subiterations of the potential because the latter is more sensitive to errors originating from approximate factorization (which can be reduced through subiterations).

It is deemed sometimes necessary to limit the electric field used to compute the Townsend ionization source terms in order to prevent the solution to diverge towards aphysical states at high CFL numbers. The approach recommended is to limit the electric field such that the resulting current density (proportional to the product of the electric field and the conductivity) does not exceed a certain user-specified value:

$$E^\star = \frac{1}{N}\left(\sum_{i=1}^{3}\left(\frac{\min\left(J_{\max},\;\max\left(-J_{\max},\;\mathrm{minmod}\left((\sigma \boldsymbol{E}_i)_{X_i-1/2},(\sigma \boldsymbol{E}_i)_{X_i+1/2}\right)\right)\right)}{\max\left(\sigma_{X_{i-1/2}},\sigma_{X_{i+1/2}}\right)}\right)^2\right)^{\frac{1}{2}} \tag{53}$$

where $E^\star$ is the reduced electric field used to determine the Townsend ionization reaction rates, N is the total number density of the plasma (including neutrals), and $J_{\max}$ is a user-specified maximum current which is typically set to about 3 times the expected maximum current density within the domain. Also, the minmod function returns the argument with the lowest magnitude, and X_i refers to the grid index along the ith dimension (i.e. $X_i - 1/2$ refers to the interface just ahead of the node under consideration along the ith dimension). It is emphasized that such a limitation of the electric field is only performed when computing the Townsend ionization terms, and does not affect the converged solution as long as the user-specified $J_{\max}$ is higher than $\sigma|\boldsymbol{E}|$ at any location within the converged solution.

TABLE 3.
Ion and electron mobilities in dry air.[a]

Charged species	Mobility, $m^2 \cdot V^{-1} \cdot s^{-1}$	Reference
Air^+	$N^{-1} \cdot \min\left(0.84 \cdot 10^{23} \cdot T^{-0.5},\ 2.35 \cdot 10^{12} \cdot (E^\star)^{-0.5}\right)$	[27][b]
N_2^+	$N^{-1} \cdot \min\left(0.75 \cdot 10^{23} \cdot T^{-0.5},\ 2.03 \cdot 10^{12} \cdot (E^\star)^{-0.5}\right)$	[27]
O_2^+	$N^{-1} \cdot \min\left(1.18 \cdot 10^{23} \cdot T^{-0.5},\ 3.61 \cdot 10^{12} \cdot (E^\star)^{-0.5}\right)$	[27]
O_2^-	$N^{-1} \cdot \min\left(0.97 \cdot 10^{23} \cdot T^{-0.5},\ 3.56 \cdot 10^{19} \cdot (E^\star)^{-0.1}\right)$	[28]
e^-	$N^{-1} \cdot 3.74 \cdot 10^{19} \cdot \exp\left(33.5 \cdot (\ln T_e)^{-0.5}\right)$	[21, Ch. 21][c]

[a] Notation and units: T_e is in Kelvin; T is in Kelvin; N is the total number density of the plasma in $1/m^3$; $E^\star$ is the reduced effective electric field ($E^\star \equiv |\boldsymbol{E}|/N$) in units of $V \cdot m^2$.

[b] The "air ion" mobility is obtained from the N_2^+ and O_2^+ ion mobilities assuming a N_2^+:O_2^+ ratio of 4:1.

[c] The expression approximates the data given in Chapter 21 of Ref. [21]; The equation can be used in the range 1000 K $\leq T_e \leq$ 57900 K with a relative error on the mobility not exceeding 20%. In the range 287 K $\leq T_e <$ 1000 K, the relative error is less than 30%.

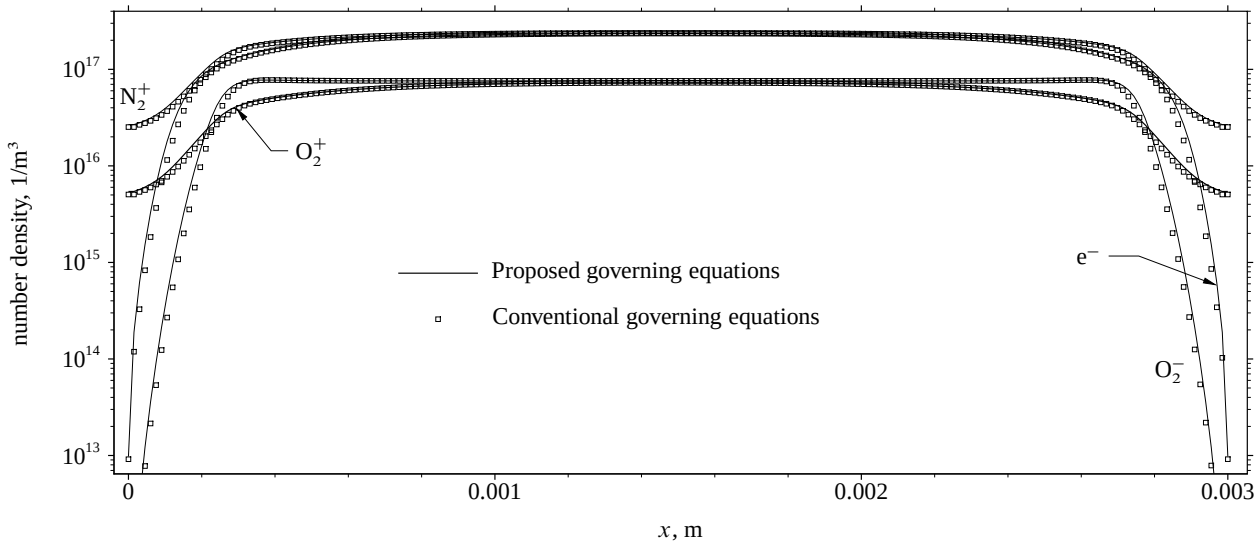

FIGURE 1. Number density profiles for the 1D multicomponent test case between two dielectrics; the grid is composed of 200 equally spaced nodes for both the proposed and conventional governing equations.

8. Test Cases

We now consider several test cases to assess the performance of the proposed governing equations. Specifically, because quasi-neutral regions are particularly difficult to solve, emphasis is put on assessing the gains in convergence acceleration when using the proposed set of equations for some plasma flow fields that include quasi-neutral regions. As well, because the gains in convergence acceleration may be accompanied by a loss of resolution, some emphasis is put on determining whether the proposed transport equations achieve as high a resolution as the conventional equations for some key plasma problems. The performance is first assessed for a multicomponent plasma (including several positive ion species and some negative ion species as well) in 1D. This is followed by a two-dimensional test case.

8.1. 1D Multicomponent Plasma

Consider first an electron-beam ionized multicomponent air plasma in 1D composed of N_2^+, O_2^+, O_2^-, e^-, N_2 and O_2. The electron temperature is fixed to 20,000 K, the N_2 number density to 1.93×10^{24} m^{-3}, the O_2 number density to 4.83×10^{23} m^{-3}, and the mobilities of the various charged species are taken from Table 3. For simplicity, the chemical reactions are limited to those listed in Table 2 and do not involve dissociated species or excited species (as in Ref. [5] for instance). Adding more

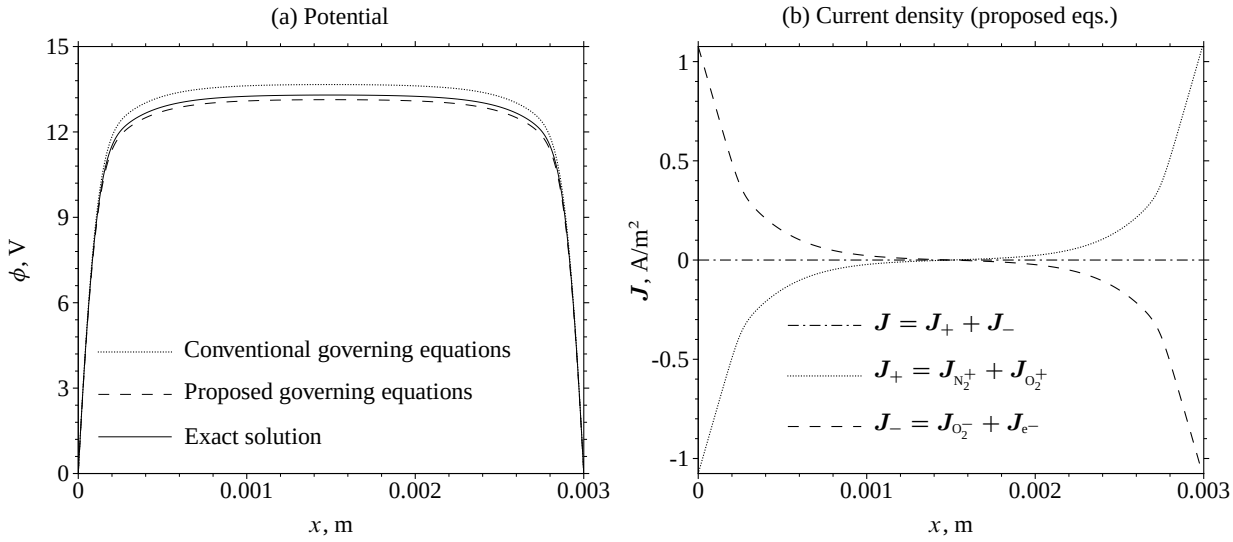

FIGURE 2. Potential and current density components for the 1D multicomponent test case using a mesh of 400 equally-spaced nodes; (a) electric field potential with the "exact" solution obtained using the conventional equations and a mesh of 1600 nodes (when using 1600 nodes, negligible differences are observed between the proposed and conventional equations); (b) current density components using the proposed equations.

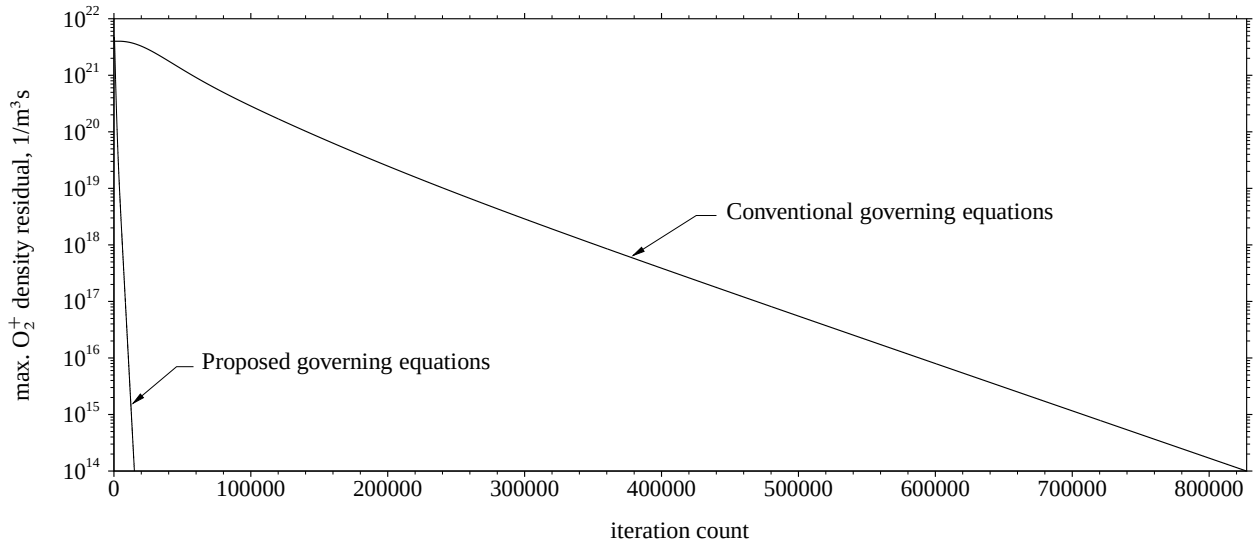

FIGURE 3. Residual history for the 1D multicomponent test case between two dielectrics; the grid is composed of 200 equally spaced nodes for both the proposed and conventional governing equations; the CFL number is fixed to 0.5 in both cases.

chemical reactions is not expected to yield significant differences for the test case under consideration and would complicate the physical model unnecessarily. The domain is 1 cm long with the left and right boundaries set to dielectrics, where the secondary emission coefficient γ is set to 0.1. Because the density of the negative ions and electrons is within the same range as the one of the positive ions, such a problem serves as a capable test case to evaluate the performance of the proposed governing equations in simulating multicomponent plasmas where negative ions play an important role. Due to the electron beam power deposited being set to an appreciable value of 10^5 W/m^3, a quasi-neutral region forms in the middle of the domain accompanied by an ambipolar diffusion region near the surfaces (see the number density profiles in Fig. 1). As can be observed from Fig. 2 and as expected from theoretical considerations, the current due to the negative species cancels out the current due to the positive species and the potential drop in Volts through the ambipolar diffusion region is in the same order of magnitude as the electron temperature in electronvolts (here $T_e = 20000\,\mathrm{K} = 1.72\,\mathrm{eV}$). When using a grid composed of 200 equally-spaced nodes, a CFL number of 0.5 combined with a length scale L_c of 1000 m is found to yield the fastest convergence for both the proposed and

TABLE 4.
Relative error assessment in solving the 1D test case at steady-state.[a,b]

Governing equations	Average relative error					
	$\frac{1}{LN_{\text{ref}}}\int_0^L \lvert N_e - (N_e)_{\text{exact}}\rvert \, \mathrm{d}x$			$\frac{1}{L\phi_{\text{ref}}}\int_0^L \lvert \phi - \phi_{\text{exact}}\rvert \, \mathrm{d}x$		
	100 nodes	200 nodes	400 nodes	100 nodes	200 nodes	400 nodes
Proposed	2.3%	0.56%	0.13%	1.8%	0.47%	0.12%
Conventional	5.4%	1.8%	0.56%	3.7%	1.2%	0.38%

[a] The "exact" solution is obtained using the proposed governing equations on a grid composed of 1600 equally-spaced nodes.
[b] The domain length L is set to 3 mm, the reference ion number density N_{ref} is set to $10^{17}/\text{m}^3$, and the reference potential ϕ_{ref} is set to 100 V.

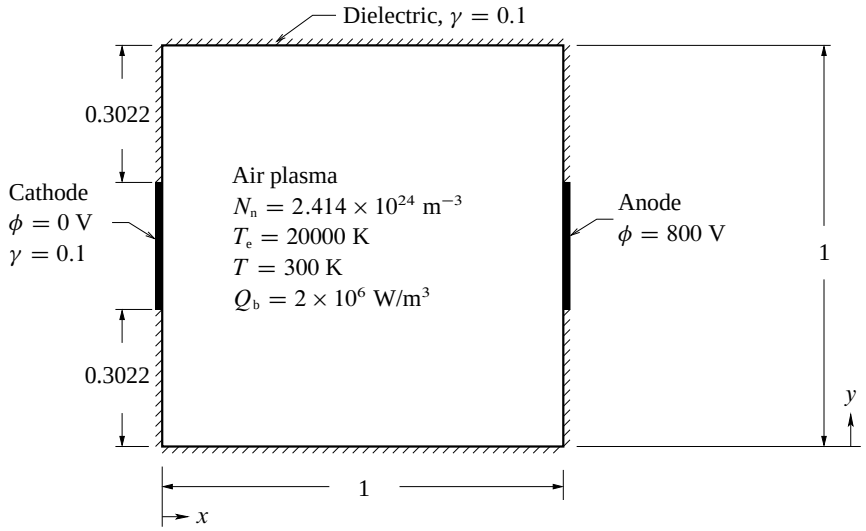

FIGURE 4: Problem setup for the two-dimensional glow discharge test case; all dimensions in millimeters.

the conventional governing equations. As attested by the residual histories shown in Fig. 3, the use of the proposed governing equations results in a substantial fiftyfold decrease in the number of iterations to reach convergence. The slow convergence of the conventional governing equations is due to the potential being obtained from Gauss's law amplifying the relative error of the number densities when the plasma is quasi-neutral (see Ref. [6] for a more thorough discussion on this point). Such an error amplification is avoided by obtaining the potential from Ohm's law as is the case when using the proposed governing equations, hence resulting in a large decrease in computing time to reach convergence. Further, not only does the proposed set of equations result in fewer iterations to reach convergence, but it does so by exhibiting a higher resolution (a higher resolution here implies a lower numerical error on a given mesh). Indeed, as outlined in Table 4, a grid convergence study indicates that the relative error is reduced 2-4 times when using the proposed set of equations. This is not due to a difference in discretization strategies: for both approaches, the same stencils are used to discretize the convection, diffusion, and source terms. Rather, the higher resolution of the proposed equations is attributed to some of the convection terms being recast in ambipolar diffusion form, hence minimizing the large discretization error that is associated to a physical situation where some of the diffusion terms cancel out the convection terms, as is the case with ambipolar diffusion.

8.2. 2D Glow Discharge

The second test case consists of a two-dimensional glow discharge in air under strong electron beam ionization with an abnormal current density regime. The air plasma is composed of 3 components: positive "air" ions, electrons, and neutrals. The mobilities are taken from Table 3 and the chemical reactions are taken from Table 1. The domain dimensions and the boundary conditions are as depicted in Fig. 4, and are such that a glow discharge takes place between the two electrodes with a substantial quasi-

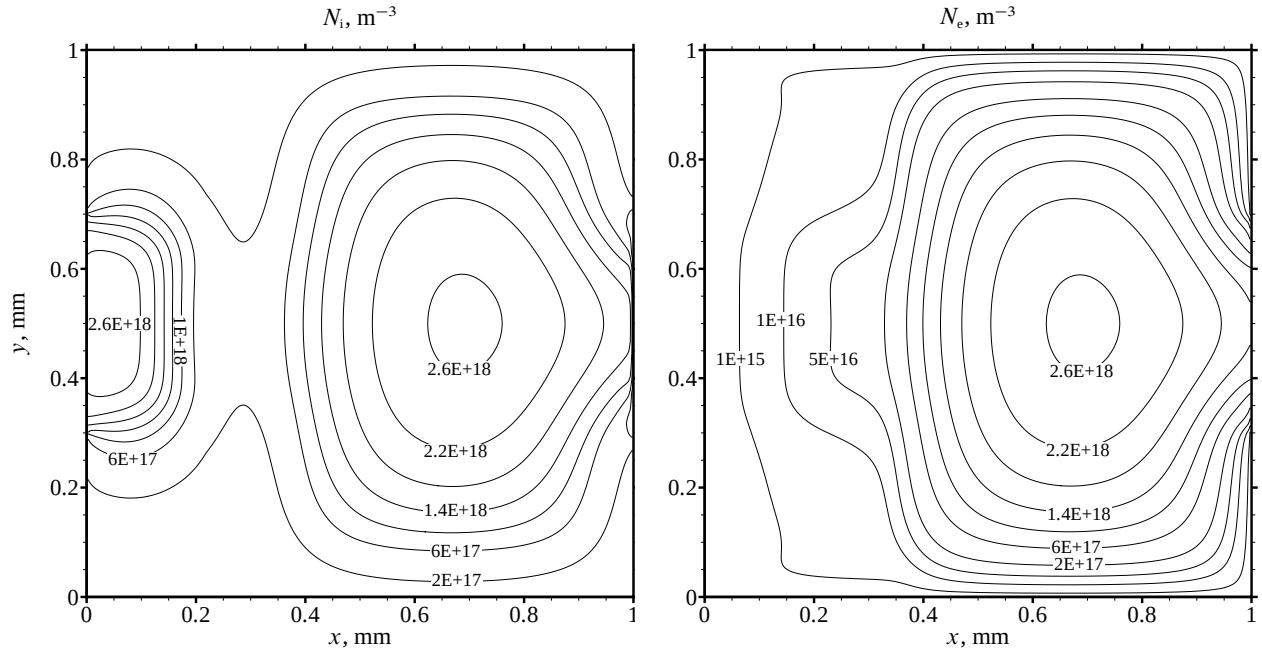

FIGURE 5. Ion and electron number density contours for the 2D glow discharge test case obtained using the proposed equations and a 345×345 mesh.

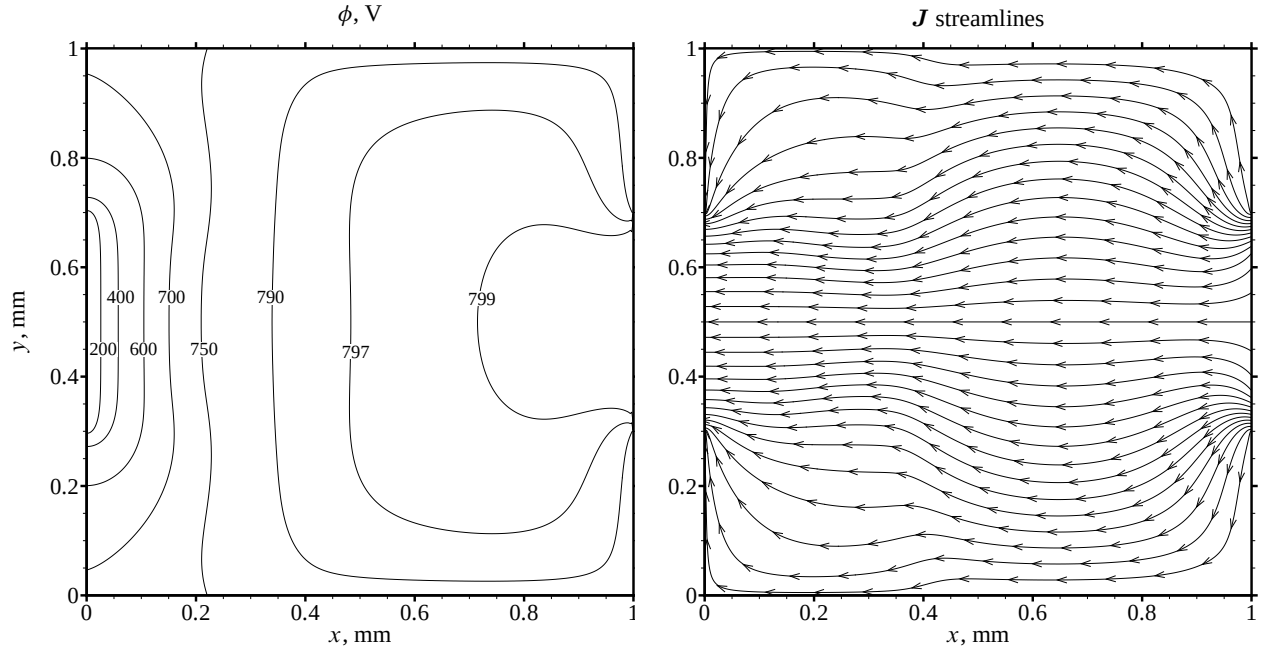

FIGURE 6. Potential contours and current density streamlines for the 2D glow discharge test case obtained using the proposed equations and a 345×345 mesh.

neutral region near the anode due to the strong e-beam power deposited (see the electron and ion density contours in Fig. 5), with most of the potential drop being located near the cathode (see Fig. 6). Such serves as a good test case to assess the performance of the proposed equations when simulating 2D cathode sheaths and anode sheaths in conjunction with a quasi-neutral region of substantial size. The characteristic length L_c on which the pseudotime step of the potential equation depends is varied cyclically as follows: 0.5 mm, 5 mm, 50 mm, 0.5 mm, 5 mm, etc. Further, to keep the solution within physical bounds, it is found necessary to perform 3 subiterations of the potential equation for each iteration of the charged species transport equations. In Fig. 7, the electron density maximum residual is plotted as a function of the iteration count for both sets of governing equations. The CFL number is adjusted in each case such as to yield the fastest possible convergence: it is first set to

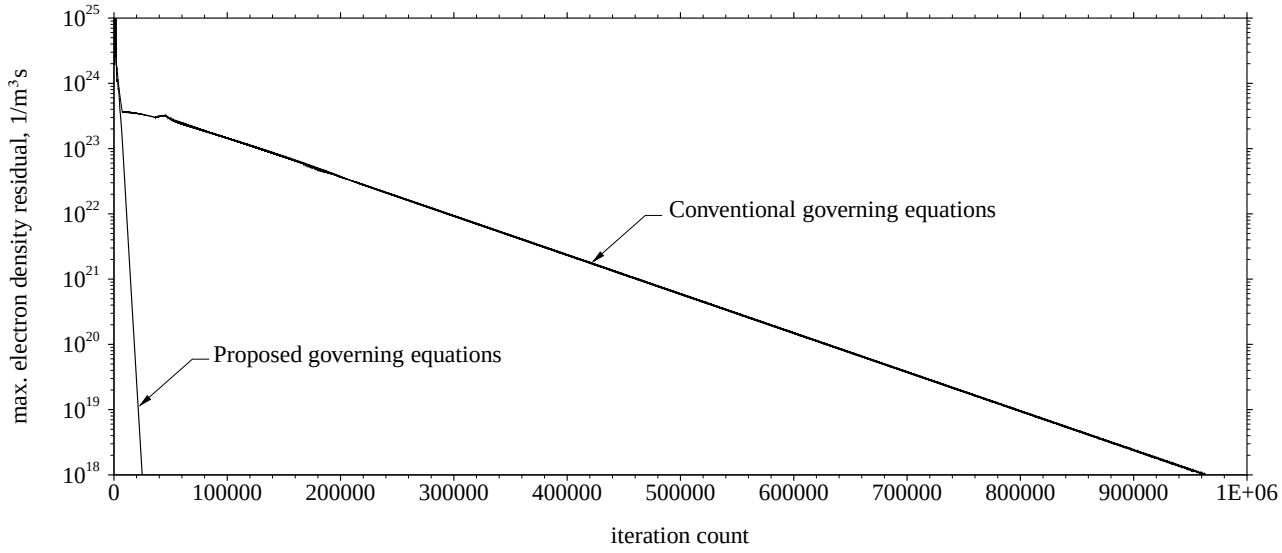

FIGURE 7. Maximum electron density residual versus the iteration count for the 2D glow discharge test case; the mesh is composed of 87×87 equally spaced nodes for both the proposed and conventional governing equations; the CFL number is fixed such as to result in the fastest convergence possible (i.e. the CFL is set initially to 10 and is raised at a rate of 0.4% each iteration until it reaches 2000 for the proposed equations and until it reaches 40 for the conventional equations).

10, and then increased at a rate of 0.4% per iteration until it reaches 40 for the conventional equations or 2000 for the proposed equations. Increasing the CFL number further would either lead to slower convergence or to divergence towards aphysical states. As can be seen from the convergence histories, a fourtyfold decrease in the number of iterations is achieved when using the proposed set of equations. Such a large difference in the amount of iterations needed to reach convergence is not due to a different integration strategy used: in both cases, the convection, diffusion and source terms are all treated implicitly and the Townsend ionization source terms are linearized in the same manner as specified above in Section 7. The slow convergence of the conventional equations is rather due to the error amplification within the potential equation based on Gauss's law preventing the CFL number from being raised substantially in quasi-neutral regions. When using the proposed equations in which the potential is obtained from Ohm's law, there is no such error amplification and the CFL number can be raised to values 50 times higher (or more), hence yielding substantial gains in convergence acceleration. It is emphasized that such gains in convergence acceleration are not accompanied by a decrease in resolution. In fact, the use of the proposed equations is found to sometimes result in an *increase* in resolution in regions where ambipolar diffusion plays an important role. For instance, a grid convergence study of the current density contours for the glow discharge test case under consideration (see Fig. 8) reveals that the proposed equations can achieve the same resolution as the conventional equations using a mesh made of 2-4 times fewer grid points. For this problem, not only does the present approach yield benefits in terms of convergence acceleration, but it also yields benefits in terms of resolution of the converged solution, therefore resulting in much improved computational efficiency.

When solved using iterative methods such as the pseudotime stepping block-implicit algorithm employed herein, glow discharge problems are well known to be particularly sensitive to the initial conditions: should the number densities be set initially to values differing too significantly from the converged solution, divergence towards aphysical states may ensue. To determine the sensitivity of the convergence to the initial conditions for the glow discharge shown herein, the initial electron and the initial ion densities are varied over the range $0 < N_e < 10^{18}$ m^{-3} and $0 < N_i < 10^{18}$ m^{-3}. Varying the initial number densities in this manner is found not to result in a substantial change in the number of iterations needed for convergence, either for the conventional or for the proposed governing equations.

Nonetheless, further investigation reveals that the initial conditions can have a substantial impact on the convergence characteristics for different glow discharge problems. For instance, consider the same geometry and same conditions as presented in Fig. 4, but with the electron beam power deposited set to zero and with the voltage difference between the anode and the cathode set to 1800 V instead of 800 V. When solving such a case to steady-state using a pseudotime iterative approach, the values given initially to the ion and electron densities are found to affect the convergence behavior significantly. For the proposed governing equations, it is deemed necessary to set the initial electron or ion densities higher than 2×10^{12} m^{-3} or the solution continuously oscillates without converging. For the conventional governing equations, it is deemed necessary to set the initial electron or ion

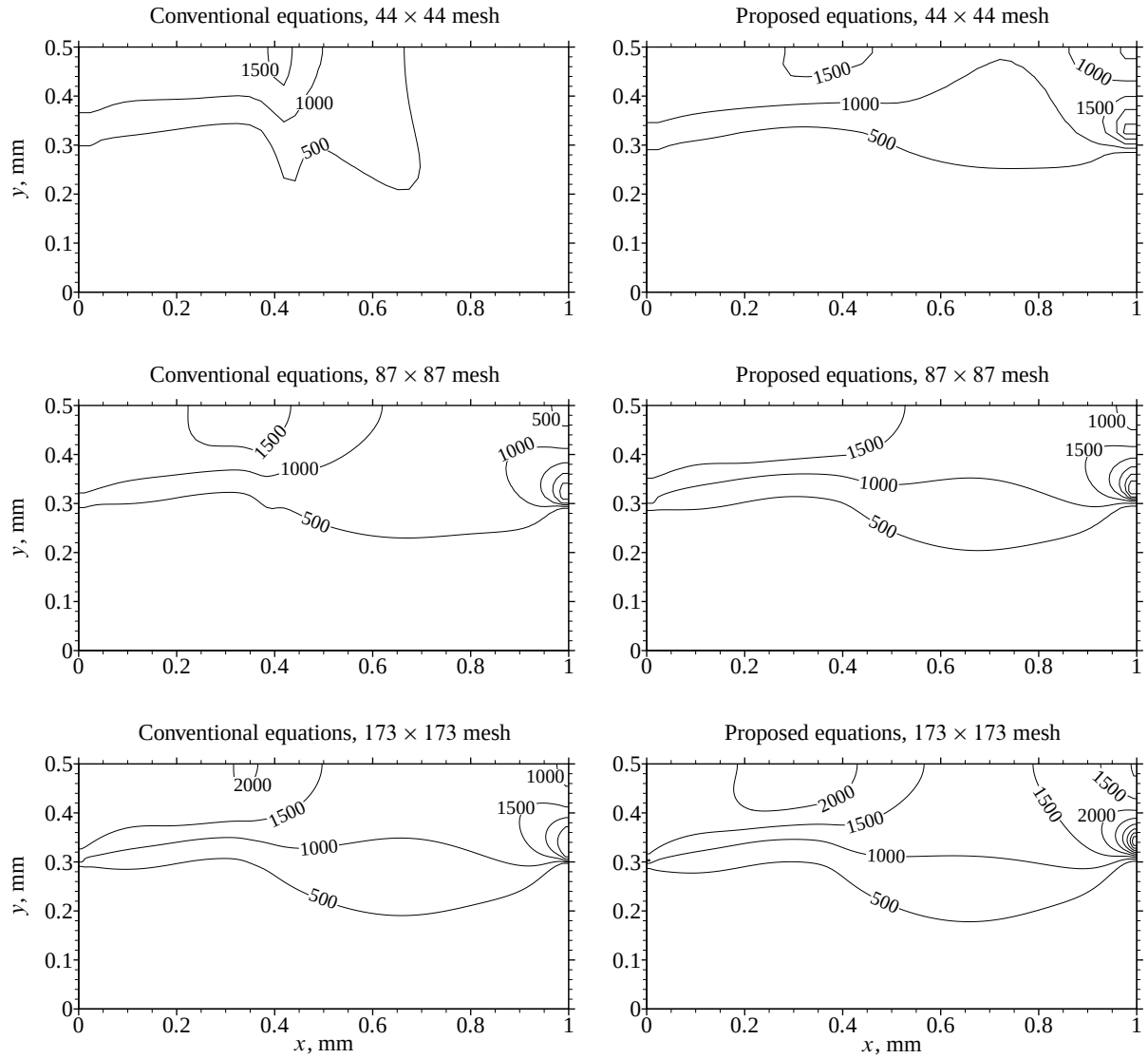

FIGURE 8. Comparison between the proposed and conventional equations on the basis of current density contours ($|\boldsymbol{J}|$ in Amps per square meter) for the glow discharge test case using various grids.

densities lower than 10^{19} m^{-3} or the solution diverges towards aphysical states. Interestingly, the proposed equations do not converge when the initial densities are set too low but do not exhibit any convergence problem when the initial densities are set too high. On the other hand, the standard equations exhibit the opposite behaviour by diverging towards aphysical states only when the initial densities are set to too high values. Several other test cases yield a similar conclusion: although the use of the present approach may affect the range of adequate initial densities, such has both advantages and disadvantages over the conventional approach and is not a particular source of concern because the range of initial densities is not overly restrictive.

9. Conclusions

A new formulation of the electron and ion transport equations is presented to simulate steady or unsteady quasi-neutral or non-neutral weakly-ionized multicomponent plasmas in multiple dimensions through the drift-diffusion approximation. The proposed transport equations differ from the standard ones by being integratable alongside a potential equation based on Ohm's law rather than Gauss's law. The proposed governing equations are obtained from the standard set without making any assumption or simplification. As such, they yield the same solution when the grid is refined sufficiently and can predict the whole range of phenomena taking place within weakly-ionized plasmas including quasi-neutral effects (ambipolar drift, ambipolar diffusion), non-neutral effects (cathode sheaths, anode sheaths, dielectric sheaths), unsteady effects where the displacement

current is significant, etc.

Because the charged species transport equations presented herein can be solved in conjunction with a potential based on Ohm's law rather than Gauss's law, they do not suffer from very slow convergence in quasi-neutral regions. Several test cases (including high current glow discharges and currentless plasmas enclosed by dielectrics) indicate that the proposed approach typically result in a 10-100 times decrease in computational effort whenever the plasma includes a quasi-neutral region of substantial size. Other test cases show that, when no quasi-neutral region is present, both sets of equations converge at a similar rate.

Several grid convergence studies confirm that such gains in convergence acceleration are obtained while not sacrificing on the resolution of the converged solution. When simulating glow discharges or other highly non-neutral plasmas in which ambipolar diffusion or drift do not play a dominant role, the solution obtained with the proposed set of equations exhibits a numerical error not greater than the one obtained using the standard set. When simulating plasmas in which ambipolar diffusion plays an important role (such as currentless quasi-neutral plasmas enclosed by dielectrics), the present approach exhibits a resolution that is significantly higher than the standard one. That is, a solution obtained with the proposed equations on a coarse mesh is as accurate as the one obtained with the conventional equations on a finer mesh. This gain in resolution is attributed to the electron transport being rewritten in ambipolar form and, therefore, exhibiting less numerical error within plasma regions in which ambipolar diffusion is significant.

The proposed recast of the electron and ion transport equations is advantaged over previous formulations by being compatible with the boundary conditions commonly used in plasmadynamics. In a previous paper, it was found necessary to reformulate the boundary conditions at the anode in order to ensure that Gauss's law would be satisfied within the anode sheath should the potential equation be obtained from Ohm's law. Such is not necessary with the present set of equations: exactly the same boundary conditions that are commonly used can be specified and no problem is encountered either at the anode, the cathode, or at the surface of dielectrics.

Because the proposed equations are not intrinsically linked to specific discretization or integration schemes and exhibit substantial advantages with no apparent disadvantage, they are generally recommended as a substitute to the current fluid models in which the electric field is obtained from Gauss's law as long as the plasma remains weakly-ionized and unmagnetized.

Acknowledgment

This research was supported by the Basic Science Research Program through the National Research Foundation of Korea (NRF) funded by the Ministry of Education, Science and Technology (Grant #2010-0023957).

A. Proof of Enforcement of Gauss's Law

It may be argued that, because the electric field is obtained from a potential equation based on Ohm's law rather than Gauss's law, Gauss's law is not necessarily satisfied when solving the set of governing equations proposed in this paper. However, it is emphasized that the proposed approach necessarily guarantees that Gauss's law is satisfied through the addition of some appropriate source terms to the positive ion transport equation. This can be better understood by considering a simple 1D problem with no negative ions, no temperature gradients, zero neutrals velocity, and only one type of positive ion. Then, the proposed ion and electron transport equations (35) simplify to:

$$R_{\mathrm{i}} = \frac{\partial N_{\mathrm{i}}}{\partial t} + E\frac{\partial}{\partial x}\left(\mu_{\mathrm{i}} N_{\mathrm{i}}\right) - \frac{\partial}{\partial x}\left(D_{\mathrm{i}}\frac{\partial N_{\mathrm{i}}}{\partial x}\right) - W_{\mathrm{i}} + \mu_{\mathrm{i}} N_{\mathrm{i}}\frac{e}{\epsilon_0}(N_{\mathrm{i}} - N_{\mathrm{e}}) \tag{A.1}$$

$$R_{\mathrm{e}} = \frac{e\mu_{\mathrm{i}} N_{\mathrm{i}}}{\sigma}\frac{\partial N_{\mathrm{e}}}{\partial t} + \frac{e\mu_{\mathrm{e}} N_{\mathrm{e}}}{\sigma}\frac{\partial N_{\mathrm{i}}}{\partial t} - J\frac{\partial}{\partial x}\left(\frac{\mu_{\mathrm{e}} N_{\mathrm{e}}}{\sigma}\right) - \frac{\partial}{\partial x}\left(\frac{e\mu_{\mathrm{e}} N_{\mathrm{e}} D_{\mathrm{i}}}{\sigma}\frac{\partial N_{\mathrm{i}}}{\partial x}\right) - \frac{\partial}{\partial x}\left(\frac{e\mu_{\mathrm{i}} N_{\mathrm{i}} D_{\mathrm{e}}}{\sigma}\frac{\partial N_{\mathrm{e}}}{\partial x}\right) - W_{\mathrm{e}} \tag{A.2}$$

and the potential equation based on Ohm's law (34) simplifies to:

$$R_\phi = \frac{\partial}{\partial t} e(N_{\mathrm{i}} - N_{\mathrm{e}}) + \frac{\partial}{\partial x}\left(-\sigma\frac{\partial \phi}{\partial x} - eD_{\mathrm{i}}\frac{\partial N_{\mathrm{i}}}{\partial x} + eD_{\mathrm{e}}\frac{\partial N_{\mathrm{e}}}{\partial x}\right) \tag{A.3}$$

where e is the elementary charge, where the subscript "e" refers the electron species and the subscript "i" to the positive ion species, where R_{e}, R_{i}, R_ϕ are the residuals that we seek to minimize through an iterative method, and where the diffusion coefficients correspond to:

$$D_{\mathrm{i}} \equiv \frac{\mu_{\mathrm{i}} k_{\mathrm{B}} T_{\mathrm{i}}}{e} \quad \text{and} \quad D_{\mathrm{e}} \equiv \frac{\mu_{\mathrm{e}} k_{\mathrm{B}} T_{\mathrm{e}}}{e} \tag{A.4}$$

Multiply Eq. (A.3) by $(\mu_i N_i)/\sigma$, add to (A.2), and simplify:

$$\begin{aligned}\frac{\mu_i N_i}{\sigma} R_\phi + R_e = \frac{\partial N_i}{\partial t} - J\frac{\partial}{\partial x}\left(\frac{\mu_e N_e}{\sigma}\right) - \frac{\partial}{\partial x}\left(\frac{e\mu_e N_e D_i}{\sigma}\frac{\partial N_i}{\partial x}\right) - \frac{\partial}{\partial x}\left(\frac{e\mu_i N_i D_e}{\sigma}\frac{\partial N_e}{\partial x}\right) \\ - W_e + \frac{\mu_i N_i}{\sigma}\frac{\partial}{\partial x}\left(-\sigma\frac{\partial\phi}{\partial x} - eD_i\frac{\partial N_i}{\partial x} + eD_e\frac{\partial N_e}{\partial x}\right)\end{aligned} \tag{A.5}$$

Substract the latter from Eq. (A.1), simplify noting that $E = -\partial\phi/\partial x$ and that $W_i = W_e$ because no net charge can be created or destroyed through the chemical reactions:

$$\begin{aligned}R_i - \frac{\mu_i N_i}{\sigma} R_\phi - R_e = E\frac{\partial}{\partial x}(\mu_i N_i) + \mu_i N_i\frac{e}{\epsilon_0}(N_i - N_e) + J\frac{\partial}{\partial x}\left(\frac{\mu_e N_e}{\sigma}\right) - \frac{\mu_i N_i}{\sigma}\frac{\partial}{\partial x}(\sigma E) - \frac{\partial}{\partial x}\left(D_i\frac{\partial N_i}{\partial x}\right) \\ + \frac{\partial}{\partial x}\left(\frac{e\mu_e N_e D_i}{\sigma}\frac{\partial N_i}{\partial x}\right) + \frac{e\mu_i N_i}{\sigma}\frac{\partial}{\partial x}\left(D_i\frac{\partial N_i}{\partial x}\right) + \frac{\partial}{\partial x}\left(\frac{e\mu_i N_i D_e}{\sigma}\frac{\partial N_e}{\partial x}\right) - \frac{\mu_i N_i}{\sigma}\frac{\partial}{\partial x}\left(eD_e\frac{\partial N_e}{\partial x}\right)\end{aligned} \tag{A.6}$$

Regroup the 5th term with the 7th term on the RHS noting that $\sigma = e\mu_i N_i + e\mu_e N_e$:

$$\begin{aligned}R_i - \frac{\mu_i N_i}{\sigma} R_\phi - R_e = E\frac{\partial}{\partial x}(\mu_i N_i) + \mu_i N_i\frac{e}{\epsilon_0}(N_i - N_e) + J\frac{\partial}{\partial x}\left(\frac{\mu_e N_e}{\sigma}\right) - \frac{\mu_i N_i}{\sigma}\frac{\partial}{\partial x}(\sigma E) \\ + \frac{\partial}{\partial x}\left(\frac{e\mu_e N_e D_i}{\sigma}\frac{\partial N_i}{\partial x}\right) - \frac{e\mu_e N_e}{\sigma}\frac{\partial}{\partial x}\left(D_i\frac{\partial N_i}{\partial x}\right) + \frac{\partial}{\partial x}\left(\frac{e\mu_i N_i D_e}{\sigma}\frac{\partial N_e}{\partial x}\right) - \frac{\mu_i N_i}{\sigma}\frac{\partial}{\partial x}\left(eD_e\frac{\partial N_e}{\partial x}\right)\end{aligned} \tag{A.7}$$

Note that the current J corresponds to:

$$J = \sigma E - eD_i\frac{\partial N_i}{\partial x} + eD_e\frac{\partial N_e}{\partial x} \tag{A.8}$$

Substitute the latter in the former:

$$\begin{aligned}R_i - \frac{\mu_i N_i}{\sigma} R_\phi - R_e = E\frac{\partial}{\partial x}(\mu_i N_i) + \mu_i N_i\frac{e}{\epsilon_0}(N_i - N_e) + \sigma E\frac{\partial}{\partial x}\left(\frac{\mu_e N_e}{\sigma}\right) - \frac{\mu_i N_i}{\sigma}\frac{\partial}{\partial x}(\sigma E) \\ - eD_i\frac{\partial N_i}{\partial x}\frac{\partial}{\partial x}\left(\frac{\mu_e N_e}{\sigma}\right) + \frac{\partial}{\partial x}\left(\frac{e\mu_e N_e D_i}{\sigma}\frac{\partial N_i}{\partial x}\right) - \frac{e\mu_e N_e}{\sigma}\frac{\partial}{\partial x}\left(D_i\frac{\partial N_i}{\partial x}\right) \\ + eD_e\frac{\partial N_e}{\partial x}\frac{\partial}{\partial x}\left(\frac{\mu_e N_e}{\sigma}\right) + \frac{\partial}{\partial x}\left(\frac{e\mu_i N_i D_e}{\sigma}\frac{\partial N_e}{\partial x}\right) - \frac{\mu_i N_i}{\sigma}\frac{\partial}{\partial x}\left(eD_e\frac{\partial N_e}{\partial x}\right)\end{aligned} \tag{A.9}$$

But, note that the following holds:

$$\frac{\partial}{\partial x}\left(\frac{\sigma}{\sigma}\right) = 0 = e\frac{\partial}{\partial x}\left(\frac{\mu_i N_i}{\sigma}\right) + e\frac{\partial}{\partial x}\left(\frac{\mu_e N_e}{\sigma}\right) \tag{A.10}$$

Isolate the second term on the RHS of the latter and substitute within the 8th term on the RHS of the former:

$$\begin{aligned}R_i - \frac{\mu_i N_i}{\sigma} R_\phi - R_e = E\frac{\partial}{\partial x}(\mu_i N_i) + \mu_i N_i\frac{e}{\epsilon_0}(N_i - N_e) + \sigma E\frac{\partial}{\partial x}\left(\frac{\mu_e N_e}{\sigma}\right) - \frac{\mu_i N_i}{\sigma}\frac{\partial}{\partial x}(\sigma E) \\ - eD_i\frac{\partial N_i}{\partial x}\frac{\partial}{\partial x}\left(\frac{\mu_e N_e}{\sigma}\right) + \frac{\partial}{\partial x}\left(\frac{e\mu_e N_e D_i}{\sigma}\frac{\partial N_i}{\partial x}\right) - \frac{e\mu_e N_e}{\sigma}\frac{\partial}{\partial x}\left(D_i\frac{\partial N_i}{\partial x}\right) \\ - eD_e\frac{\partial N_e}{\partial x}\frac{\partial}{\partial x}\left(\frac{\mu_i N_i}{\sigma}\right) + \frac{\partial}{\partial x}\left(\frac{e\mu_i N_i D_e}{\sigma}\frac{\partial N_e}{\partial x}\right) - \frac{e\mu_i N_i}{\sigma}\frac{\partial}{\partial x}\left(D_e\frac{\partial N_e}{\partial x}\right)\end{aligned} \tag{A.11}$$

After expanding the second term on the second line and the second term on the third line, and simplifying, we get:

$$R_i - \frac{\mu_i N_i}{\sigma} R_\phi - R_e = E\frac{\partial}{\partial x}(\mu_i N_i) + \mu_i N_i\frac{e}{\epsilon_0}(N_i - N_e) + \sigma E\frac{\partial}{\partial x}\left(\frac{\mu_e N_e}{\sigma}\right) - \frac{\mu_i N_i}{\sigma}\frac{\partial}{\partial x}(\sigma E) \tag{A.12}$$

Expand the last term on the RHS:

$$R_i - \frac{\mu_i N_i}{\sigma} R_\phi - R_e = E\frac{\partial}{\partial x}(\mu_i N_i) + \mu_i N_i\frac{e}{\epsilon_0}(N_i - N_e) + \sigma E\frac{\partial}{\partial x}\left(\frac{\mu_e N_e}{\sigma}\right) - \mu_i N_i\frac{\partial E}{\partial x} - \frac{E\mu_i N_i}{\sigma}\frac{\partial\sigma}{\partial x} \tag{A.13}$$

Expand the 3rd term on the RHS as follows:

$$\sigma E\frac{\partial}{\partial x}\left(\frac{\mu_e N_e}{\sigma}\right) = E\frac{\partial}{\partial x}(\mu_e N_e) - E\frac{\mu_e N_e}{\sigma}\frac{\partial\sigma}{\partial x} \tag{A.14}$$

Substitute the latter in the former, and simplify noting that $\sigma = e(\mu_\mathrm{i} N_\mathrm{i} + \mu_\mathrm{e} N_\mathrm{e})$:

$$R_\mathrm{i} - \frac{\mu_\mathrm{i} N_\mathrm{i}}{\sigma} R_\phi - R_\mathrm{e} = \mu_\mathrm{i} N_\mathrm{i} \left(\frac{e}{\epsilon_0}(N_\mathrm{i} - N_\mathrm{e}) - \frac{\partial E}{\partial x} \right) \tag{A.15}$$

Note that when the set of equations (A.1)–(A.3) is converged, the residuals become zero: $R_\mathrm{i} \to 0$, $R_\mathrm{e} \to 0$, and $R_\phi \to 0$. Then, from Eq. (A.15), this entails that solving the system (A.1)–(A.3) necessarily results in Gauss's law being satisfied. Because Gauss's law is satisfied, it can be easily shown that the solution of the modified ion transport equation (A.1) necessarily entails the solution of the standard ion transport equation. It can be further shown that this ensures the solution of the standard electron transport equation because the solved potential equation based on Ohm's law corresponds to the difference between the standard ion and electron transport equations. Thus, it is clear that Eq. (A.1) does not automatically follow from Equations (A.2) and (A.3), and therefore the system (A.1)–(A.3) is complete: there are 3 independent equations for 3 unknowns.

Although the proof presented above applies to a three-component onedimensional plasma, it can also be shown by following similar steps that the proposed approach provides enough equations for the number of unknowns and guarantees that Gauss's law is satisfied (either in quasi-neutral or non-neutral regions) for multicomponent and multidimensional weakly-ionized plasmas.

References

[1] SURZHIKOV, S., *Computational Physics of Electric Discharges in Gas Flows*, De Gruyter, Berlin, Boston, 2012.

[2] SHANG, J. S. AND HUANG, P. G., "Modeling of AC Dielectric Barrier Discharge," *Journal of Applied Physics*, Vol. 107, No. 11, 2010, pp. 113302.1–113302.7.

[3] SHANG, J. S., ROVEDA, F., AND HUANG, P. G., "Electrodynamic Force of Dielectric Barrier Discharge," *Journal of Applied Physics*, Vol. 109, No. 11, 2011, pp. 113301.1–113301.8.

[4] ATKINSON, M. D., POGGIE, J., AND CAMBEROS, J. A., "Control of Separated Flow in a Reflected Shock Interaction Using a Magnetically-Accelerated Surface Discharge," *Physics of Fluids*, Vol. 24, No. 12, 2012, pp. 126102.1–126102.17.

[5] POGGIE, J., ADAMOVICH, I., BISEK, N., AND NISHIHARA, M., "Numerical Simulation of Nanosecond-Pulse Electrical Discharges," *Plasma Sources Science and Technology*, Vol. 22, No. 1, 2013, pp. 015001.1–015001.17.

[6] PARENT, B., SHNEIDER, M. N., AND MACHERET, S. O., "Sheath Governing Equations in Computational Weakly-Ionized Plasmadynamics," *Journal of Computational Physics*, Vol. 232, No. 1, 2013, pp. 234–251.

[7] CRISPEL, P., DEGOND, P., AND VIGNAL, M.-H., "An asymptotic preserving scheme for the two-fluid Euler-Poisson model in the quasineutral limit," *Journal of Computational Physics*, Vol. 223, 2007, pp. 208–234.

[8] LIKHANSKII, A. V., SHNEIDER, M. N., MACHERET, S. O., AND MILES, R. B., "Modeling of Dielectric Barrier Discharge Plasma Actuators Driven by Repetitive Nanosecond Pulses," *Physics of Plasmas*, Vol. 14, No. 7, 2007.

[9] GRAVES, D. B. AND JENSEN, K. F., "A Continuum Model of DC and RF Discharges," *IEEE Transactions on Plasma Science*, Vol. PS-14, No. 2, 1986, pp. 78–91.

[10] SCHMITT, W., KOHLER, W. E., AND RUDER, H., "A One-Dimensional Model of DC Glow Discharges," *Journal of Applied Physics*, Vol. 71, No. 12, 1992, pp. 5783–5791.

[11] ROY, S., PANDLEY, B. P., POGGIE, J., AND GAITONDE, D. V., "Modeling Low Pressure Collisional Plasma Sheath with Space-Charge Effect," *Physics of Plasmas*, Vol. 10, No. 6, 2002, pp. 2578–2585.

[12] MACHERET, S. O., SHNEIDER, M. N., AND MILES, R. B., "Modeling of Air Plasma Generation by Repetitive High-Voltage Nanosecond Pulses," *IEEE Transactions on Plasma Science*, Vol. 30, No. 3, 2002, pp. 1301–1314.

[13] SURZHIKOV, S. T. AND SHANG, J. S., "Two-Component Plasma Model for Two-Dimensional Glow Discharge in Magnetic Field," *Journal of Computational Physics*, Vol. 199, 2004, pp. 437–464.

[14] POGGIE, J., "Numerical Simulation of Direct Current Glow Discharges for High-Speed Flow Control," *Journal of Propulsion and Power*, Vol. 24, No. 5, 2008, pp. 916–922.

[15] RAIZER, Y. P. AND SHNEIDER, M. N., "Electrodeless Capacitive Discharge Sustained by Repetitive High-Voltage Pulses," *Teplofizika Vysokikh Temperatur*, Vol. 27, No. 3, 1989, pp. 431–438, English translation.

[16] PARENT, B., SHNEIDER, M. N., AND MACHERET, S. O., "Generalized Ohm's Law and Potential Equation in Computational Weakly-Ionized Plasmadynamics," *Journal of Computational Physics*, Vol. 230, No. 4, 2011, pp. 1439–1453.

[17] RAIZER, Y. P., *Gas Discharge Physics*, Springer-Verlag, Berlin, Germany, 1991.

[18] RAIZER, Y. P., SHNEIDER, M. N., AND YATSENKO, N. A., *Radio-Frequency Capacitive Discharges*, CRC Press, U.S.A., 1995.

[19] PARENT, B., MACHERET, S. O., AND SHNEIDER, M. N., "Ambipolar Diffusion and Drift in Computational Weakly-Ionized Plasmadynamics," *Journal of Computational Physics*, Vol. 230, No. 22, 2011, pp. 8010–8027.

[20] MNATSAKANYAN, A. K. AND NAIDIS, G. V., "Processes of Formation and Decay of Charged Particles in Nitrogen-Oxygen Plasmas," *Khimiia Plazmy [Plasma Chemistry]*, edited by B. M. Smirnov, Vol. 14, Energoatomizdat, Moscow, Russia, 1987, pp. 227–255, in russian.

[21] GRIGORIEV, I. S. AND MEILIKHOV, E. Z., *Handbook of Physical Quantities*, CRC, Boca Raton, Florida, 1997.

[22] PETERSON, L. R. AND GREEN, A. E. S., "The Relation Between Ionization Yields, Cross Sections, and Loss Functions," *Journal of Physics B: Atomic, Molecular and Optical Physics*, Vol. 1, No. 6, 1968, pp. 1131–1140.

[23] KOSSYI, A., KOSTINSKY, A. Y., MATVEYEV, A. A., AND SILAKOV, V. P., "Kinetic Scheme of the Non-Equilibrium Discharge in Nitrogen-Oxygen Mixtures," *Plasma Sources Science and Technology*, Vol. 1, 1992, pp. 207–220.

[24] ALEKSANDROV, N. L., BAZELYAN, E. M., KOCHETOV, I. V., AND DYATKO, N. A., "The Ionization Kinetics and Electric Field in the Leader Channel in Long Air Gaps," *Journal of Physics D Applied Physics*, Vol. 30, 1997, pp. 1616–1624.

[25] BAZELYAN, E. M. AND RAIZER, Y. P., *Spark Discharge*, CRC, Boca Raton, Florida, 1997.

[26] BYCHKOV, Y. I., KOROLEV, Y. D., AND MESYATS, G. A., *Inzhektsionnaia Gazovaia Elektronika*, Nauka, Novosibirsk, Russia, 1982, (Injection Gaseous Electronics, in Russian).

[27] SINNOTT, G., GOLDEN, D. E., AND VARNEY, R. N., "Positive-Ion Mobilities in Dry Air," *Physical Review*, Vol. 170, No. 1, 1968, pp. 272–275.

[28] GOSHO, Y. AND HARADA, A., "A New Technique for Measuring Negative Ion Mobilities at Atmospheric Pressure," *Journal of Physics D*, Vol. 16, 1983, pp. 1159–1166.